[redacted]

Copy 274
RM E52H25



[redacted]

NACA

# RESEARCH MEMORANDUM

## EFFECT OF WATER VAPOR ON COMBUSTION OF MAGNESIUM-HYDROCARBON SLURRY FUELS IN SMALL-SCALE AFTERBURNER

By Leonard K. Tower

Lewis Flight Propulsion Laboratory
Cleveland, Ohio



[redacted]

NATIONAL ADVISORY COMMITTEE FOR AERONAUTICS
WASHINGTON
October 22, 1952

[redacted]

[redacted]

2568

NATIONAL ADVISORY COMMITTEE FOR AERONAUTICS

RESEARCH MEMORANDUM

# EFFECT OF WATER VAPOR ON COMBUSTION OF MAGNESIUM-HYDROCARBON SLURRY FUELS IN SMALL-SCALE AFTERBURNER

By Leonard K. Tower

## SUMMARY

Both JP-3 fuel and a slurry of 60 percent powdered magnesium in JP-3 fuel were evaluated in a small-scale afterburner in the presence of large quantities of water vapor. From data obtained with the small-scale afterburner, the static sea-level performance was computed for turbojet engines augmented by combined water injection and magnesium-slurry afterburning.

Combustion of 60-percent-magnesium slurry in the small-scale afterburner was stable to the highest water-air ratio investigated, 0.18. The JP-3 fuel would not burn beyond a water-air ratio of 0.08.

The following table reveals that total temperature, combustion efficiency, and air specific impulse were improved when the magnesium slurry rather than JP-3 fuel alone was used in the small-scale afterburner both with and without water vapor:

| Fuel | Water-air ratio | Afterburner total temperature[1] (°R) | Afterburner combustion efficiency[1] | Air specific impulse[1] (sec) |
|---|---|---|---|---|
| JP-3 | 0 | 3650 | 0.78 | 157 |
| | .07 | 2800 | .56 | 150 |
| Slurry | 0 | 4760 | 0.87 | 177 |
| | .12 | 3720 | .87 | 182 |

[1]Afterburner equivalence ratio of 1.0.

These improvements were at the expense of increased liquid consumption.

By means of these total-temperature data, turbojet static sea-level performance with combined water injection and afterburning was computed for two engines. One of the engines was assumed to make ideal use of injected water. In the other engine, the effectiveness of water was

assumed to be that experienced in previous experiments. Results for an afterburner equivalence ratio of 1.0 were as follows:

2568

| Type of water injection | Afterburner fuel | No water injection | | Water injection | |
|---|---|---|---|---|---|
| | | Augmented thrust ratio | Augmented liquid ratio | Maximum augmented thrust ratio | Augmented liquid ratio |
| Ideal | JP-3 | 1.47 | 4.0 | 1.81 | 6.8 |
| | Slurry | 1.75 | 6.9 | 2.15 | 9.8 |
| Experi-mental | JP-3 | 1.43 | 4.0 | 1.58 | 7.0 |
| | Slurry | 1.67 | 6.9 | 2.00 | 13.6 |

From these results it may be predicted that afterburning with 60-percent-magnesium slurry in place of JP-3 fuel may shorten the take-off distance of some aircraft 17 to 24 percent.

## INTRODUCTION

Physical and thermal properties of high-energy fuels, such as high heating value per unit volume, per unit fuel weight, or per unit air weight, offer potential increases in range or thrust of aircraft (reference 1). Fuel slurries, or suspensions of powdered metal and hydrocarbon fuels, have been proposed as a means of simplifying the storage and handling problems presented by the metallic high-energy fuels.

Small-scale afterburner tests, showing the superior thrust-producing capacity of magnesium-hydrocarbon slurries as compared with hydrocarbons alone (reference 2), make the application of magnesium slurries to aircraft afterburners appear promising. Reference 3 concludes that these slurry fuels may, with sufficient research, be given satisfactory properties such as physical stability by the use of additives.

The experiments conducted on the small-scale afterburner (reference 2) indicate that the reactivity of magnesium slurries with air exceeds that of hydrocarbon fuels alone. Under comparable conditions of burner-inlet velocity and pressure, a narrower operating region of equivalence ratio was found for hydrocarbon fuels than for magnesium slurries. A simplified flame-holder and injection-nozzle configuration, used successfully with magnesium slurry, would not secure stable combustion with the hydrocarbon fuel alone. Reference 4 substantiates the high reactivity of magnesium slurries as compared with hydrocarbons.

Analyses of combustion products taken from a small combustor burning slurries of magnesium powder in hydrocarbons reveal that when slurry fuel-air mixture is rich, the magnesium combines with the available oxygen at the expense of the hydrocarbon present.

2568 Because of their high reactivity and potential performance increases, magnesium-hydrocarbon slurries warrant consideration in applications where the use of hydrocarbon fuels results in combustion instability or inefficiency or in insufficient energy release. One such possible application is in the afterburner of a turbojet engine additionally augmented by compressor or combustion-chamber coolant injection. A theoretical analysis in reference 5 predicts a thrust augmentation with a combination of hydrocarbon afterburning and water injection which was not realized experimentally by the use of water or water-alcohol mixtures (reference 6). Among the causes for this lack of agreement are ineffective vaporization of the coolant, the detrimental effect of the coolant upon engine component performance, and the decrease in afterburner combustion efficiency and stability as increasing quantities of coolants containing water are injected.

Magnesium slurries may be more satisfactory than hydrocarbons as afterburner fuels in such a system involving concurrent water or water-alcohol injection because of the high reactivity of magnesium with both water (a constituent of some coolants) and air.

An investigation was conducted at the NACA Lewis laboratory to determine in the presence of water vapor the combustion properties of slurries containing 60 percent atomized magnesium powder and 40 percent hydrocarbon by weight. The hydrocarbon was a specially blended JP-3 fuel of low aromatic content meeting MIL-F-5624 specifications. Data reported herein were obtained with a 6-inch small-scale afterburner.

## APPARATUS AND PROCEDURE

The small-scale afterburner installation, very similar to that described in reference 3, is shown in figure 1. It consists essentially of an air-supply line, a jet-engine can-type combustor (hereafter referred to as the primary combustor) in which propane was burned to simulate turbine-outlet temperature, a length of straight duct at the downstream end of which the afterburner-inlet instrumentation was located, and an afterburner. The reaction of the exhaust jet against a barrel-type thrust target, which turned the exhaust through 90°, was used to measure thrust. The pressure in the thrust target was slightly in excess of atmospheric. The slurry fuel system, the same as that described in reference 3, is depicted in figure 2.

2568

Afterburner configuration and fuel sprays. - The air-atomizing spray bar and the afterburner configuration used in obtaining data with the JP-3 fuel are shown in figure 3. The combination represents a satisfactory combustor configuration for JP-3 fuel, which was evolved from a few trials (reference 3).

The afterburner configuration, a single water-cooled injection nozzle, and the nozzle manifold used with the 60-percent-magnesium slurry are shown in figure 4. This configuration was found in reference 3 to provide for good combustion of the slurry fuel without burning out the flame holder. Alternate wall injection nozzles were manifolded together, forming two groups of four nozzles each. At the lower fuel flow rates, one manifold was used, permitting higher injection pressures than could be obtained with a single fuel system.

Water-injection system. - Water was injected into the duct at the downstream end of the primary combustor through four atomizing fuel nozzles manifolded in groups of two as shown in figure 1. About 81 inches of duct were available for vaporization between the point of injection and the station where afterburner-inlet temperature was measured. A heat balance, based upon the primary-combustor heat input and the enthalpy rise required for complete vaporization of the water, indicated that the amount of water evaporated at the afterburner inlet varied as follows:

| Water-air ratio | Water vaporized (percent) |
|---|---|
| 0.02 | 65 |
| .03 | 73 |
| .06 | 85 |
| .09 | 89 |

The effect of the water upon performance is shown herein to be most critical beyond 0.05 water-air ratio, where 80 percent or more of the water was known to be vaporized at the burner inlet. Wet and dry bulb thermocouples indicated that the moisture content of the combustion air prior to the point of water injection was negligible.

Fuel. - The fuels evaluated were a hydrocarbon reference fuel and a blend containing 60 percent atomized magnesium and 40 percent hydrocarbon reference fuel. The hydrocarbon reference fuel met MIL-F-5624 specifications, as shown in table I, except for a minor discrepancy in vapor pressure. It was prepared to have an aromatic content of less than 10 percent. The characteristics of the magnesium powder used in the slurry blend are listed in table II.

Operating procedure. - The slurry fuel flow was computed from the calibration obtained for the hydrocarbon by the relation

2568

$$\frac{W_{b,slurry}}{W_{b,JP-3}} = \sqrt{\frac{\rho_{slurry}}{\rho_{JP-3}}}$$

(Symbols are defined in appendix A.) This procedure is verified by figure 7 of reference 3, where data for slurries containing several concentrations of magnesium are reduced to a single relation of orifice differential pressure against weight flow by the correction factor shown.

During all runs a combustion air flow of nearly 2.50 pounds per second and an afterburner-inlet temperature of 1660° R were maintained. The afterburner-inlet velocity ranged between 300 and 450 feet per second, primarily because of a variation in afterburner pressure between 16 and 24 pounds per square inch. About 2 pounds per second of cooling air was passed through the burner cooling jacket to limit maximum afterburner wall temperature to 1100° F. Because experience showed that the presence of water vapor made the ignition of JP-3 fuel difficult, the afterburner was ignited by momentary enrichment of the propane flow to the primary combustor before water injection was begun. The ignition of magnesium slurry in the presence of water vapor was not attempted. The afterburner fuel flow was held approximately constant and the quantity of water injected was progressively increased until either combustion instability or water-pump capacity was reached. Limited fuel quantity did not allow the operating time necessary for the precise setting of either water flow or afterburner fuel flow. This limitation necessitated the use of interpolation in reducing the data to fixed fuel-air ratios or water-air ratios. Unless blow-out occurred, the afterburner operated continuously throughout a series of runs. Between the adjustment of conditions for every run and the recording of data, about 30 seconds was allowed to establish thermal equilibrium; 30 seconds was also consumed in reading and recording the data. Thrust and fuel flow were recorded every 2 seconds during the data-taking interval.

## RESULTS AND DISCUSSION

### Performance of JP-3 Fuel and Magnesium Slurry in Small-Scale Afterburner

A tabulation of performance data for runs with the small-scale afterburner is presented in table III. Some of the more important data have been plotted for the purpose of discussion.

Effect of water injection on primary-combustor and afterburner fuel-air ratios. - As water-air ratio was increased, propane flow to the primary combustor was also increased to maintain afterburner-inlet temperature at 1660° R (fig. 5). The afterburner fuel to total-air ratio required for stoichiometric utilization of the remaining oxygen then decreased as shown. The afterburner equivalence ratio was thus 1.0. 2568

Effect of water injection on the stability limits of JP-3 fuel and 60-percent-magnesium slurry. - The afterburner equivalence ratio and corresponding water-air ratio for each of the runs with JP-3 fuel and with 60-percent-magnesium slurry are shown in figure 6. Stable combustion was obtained with JP-3 fuel only within the zone enclosed by the hatched line. As water-air ratio was increased, stable operation with JP-3 fuel was obtainable over a decreasing band of equivalence ratios. Beyond a water-air ratio of 0.08, flame blow-out occurred at all equivalence ratios.

The stability limits are also shown from reference 6 for a full-scale engine with JP-3 fuel in an afterburner and coolant injection in the compressor. The compressor coolant was a mixture of 75 percent water and 25 percent alcohol by weight. The coolant containing 75 percent water was detrimental to the combustion stability of the full-scale afterburner, as was water alone in the small-scale afterburner.

In none of the runs with 60-percent-magnesium slurry was combustion instability or blow-out encountered. The capacity of the water-pumping system limited the water-air ratio obtainable with 60-percent-magnesium slurry to 0.18, as shown in figure 6. With the slurry, combustion in the small-scale burner was stable at a water-air ratio of more than $2\frac{1}{4}$ times that obtainable with JP-3 fuel.

The combustion stability of the magnesium slurry in the presence of water is presumably due to the strong chemical reactivity of magnesium with water. The reaction of magnesium with water is well established and is cited in literature such as reference 7. Examination of the free energies listed in reference 8 for the reaction of water with magnesium and the reaction of oxygen with magnesium indicates that magnesium exhibits a strong chemical affinity for both the water and the oxygen contained in the combustion air. Little specific information on the kinetic rate of the reaction of powdered magnesium with water and air is available. However, the oxidation of magnesium powder in an air stream heated to 470° C, slightly below the ignition temperature, has been investigated (reference 9). Air containing a moisture concentration equivalent to the normal atmosphere gave an oxidation rate 3 times as great as dry air.

Effect of water injection on total temperatures and combustion efficiencies in the small-scale afterburner. - Total temperatures in the small-scale afterburner were computed at an equivalence ratio of 1.0 for both JP-3 fuel and 60-percent-magnesium slurry. Appendix B presents thermodynamic properties of combustion products necessary in the computation discussed in appendix C. The variation of total temperature with water-air ratio for both JP-3 fuel and 60-percent-magnesium slurry is plotted in figure 7(a). With no water injection the slurry gave a calculated total temperature of 4760° R as compared with 3650° R with JP-3 fuel. The total temperature with slurry declined to 3720° R at 0.12 water-air ratio, whereas with JP-3 it declined to 2800° R at 0.07 water-air ratio. A decrease in total temperature with increasing water-air ratio may be expected because of the decrease in the oxygen available to the afterburner and because of a possible decrease in afterburner combustion efficiency.

The effect of variation in water-air ratio upon afterburner combustion efficiency at an equivalence ratio of 1.0 for both JP-3 fuel and 60-percent-magnesium slurry is shown in figure 7(b). The method of computing combustion efficiency, defined as the ratio $\Delta H\Big]_6^8/Q_1$, is discussed in appendix C. The combustion efficiency of 60-percent-magnesium slurry remained nearly constant at values exceeding 0.87 to water-air ratios of 0.12. The JP-3 fuel gave a combustion efficiency of about 0.78 at low water-air ratios, declining to 0.56 at 0.07 water-air ratio.

Air specific impulse. - The propulsive performance of a thermodynamic duct is frequently expressed as air specific impulse (total stream momentum per pound of air). The implications and usefulness of this and other duct momentum relations are explained in reference 10. Appendix C presents the definition of air specific impulse.

Air specific impulse in a choked burner $S_a^*$ is a measure of the jet-thrust-producing capability of a fuel. The effect of water injection upon $S_a^*$ over a range of equivalence ratios for both JP-3 fuel and 60-percent-magnesium slurry is shown in figure 8. Each run is represented by a datum point with the corresponding afterburner equivalence ratio indicated by an adjacent number. Lines of constant afterburner equivalence ratio have been faired among the points. This interpolation was accomplished by the construction of a smoothed three-dimensional model of the surface involving the following coordinates: water-air ratio, equivalence ratio, and air specific impulse. At an equivalence ratio of 1.0, JP-3 gave an $S_a^*$ of 157 seconds with no water injection. The injection of water resulted in a rapid drop in $S_a^*$ beyond a water-air ratio of 0.05, reaching 150 seconds at 0.07 water-air ratio. Slurry at an equivalence ratio of 1.0 gave an $S_a^*$ of 177 seconds with no water injection, increasing to 182 seconds at a water-air ratio of 0.10.

Predicted Performance of Turbojet Engines with Combined Water Injection and Afterburning of JP-3 Fuel or Magnesium Slurry

By use of the total temperatures determined for the small-scale afterburner, the thrust augmentation resulting from afterburning of JP-3 fuel or slurry was computed for engines with and without water injection. Performance was considered for two engines, one making ideal use of injected water and the other utilizing water in an experimentally determined manner. 2568

<u>Thrust augmentation of a turbojet engine combining afterburning with ideal water-injection performance</u>. - A method of water injection which has been investigated theoretically is the introduction of the water at the compressor entrance. As the wet mixture passes through the compressor, the coolant is assumed to vaporize with sufficient ease to maintain saturation. If the coolant vaporizes completely before compression is complete, the wet compression is followed by a dry compression.

The sea-level static performance to be expected from the theoretical engine by such ideal use of water injection with and without afterburning was computed with the methods and assumptions discussed in appendix D. The afterburner total temperatures used in making the computations were those shown in figure 7 for the small-scale afterburner with JP-3 fuel or magnesium slurry.

The sea-level static performance of this engine with ideal water injection is presented in figure 9 as augmented thrust ratio (ratio of augmented to normal thrust) against augmented liquid ratio (ratio of augmented total liquid consumption to normal total liquid consumption). The afterburner is considered to be operating at an equivalence ratio of 1.0. The following table summarizes the results shown in figure 9:

| | No water injection | | Water injection | |
|---|---|---|---|---|
| | Augmented thrust ratio | Augmented liquid ratio | Maximum augmented thrust ratio | Augmented liquid ratio |
| No afterburning (curve C) | 1.00 | 1.0 | 1.29 | 4.7 |
| Afterburning with JP-3 (curve B) | 1.47 | 4.0 | 1.81 | 6.8 |
| Afterburning with slurry (curve A) | 1.75 | 6.9 | 2.15 | 9.8 |

The engine without water injection produces 19 percent more thrust with 60-percent-magnesium slurry than with JP-3 fuel. When water injection is employed, the maximum engine thrust with 60-percent-magnesium slurry again exceeds that with JP-3 fuel by 19 percent. These high values of thrust augmentation are achieved at the expense of high total liquid consumption.

2568 Thrust augmentation of a turbojet engine combining afterburning with experimental water-injection performance. - The great effectiveness of injected coolants containing water as previously described has not been obtained in practice. Mixture saturation within the compressor is not attained. The coolant must be injected in small amounts at stages through an axial-flow compressor to avoid damage resulting from centrifugal separation of the wet mixture. Such deviation from ideal processes lowers the thrust augmentation obtainable from a given quantity of coolant. The least effective method of introducing the coolant is to inject it directly into the engine combustion chambers, since no air-flow increase is experienced as is sometimes the case with compressor coolant injection.

Augmented thrust ratio is shown by curve A of figure 10 for an actual engine employing a combination of compressor interstage injection and combustion-chamber injection. These data were obtained from a previous investigation (reference 11). The coolant employed was a mixture of 75 percent water and 25 percent alcohol by weight. About 0.024 pound coolant per pound air, corresponding to an augmented liquid ratio of 2.5, was injected at the sixth stage of the compressor, and the remainder was injected in the center of the engine combustion chambers. The probability that water alone should give performance comparable to that obtained from the water-alcohol mixture at sea-level conditions is indicated in reference 12.

Computed performance is shown by curves B and C (fig. 10) for this same turbojet engine using water injection in combination with afterburning of JP-3 fuel and 60-percent-magnesium, respectively. These curves were computed from the experimental data of curve A for water-injection performance together with the small-scale afterburner results reported herein for an equivalence ratio of 1.0. The methods and assumptions of appendix D were used in the calculations. The results are summarized in the following table:

| | No water injection | | Water injection | |
|---|---|---|---|---|
| | Augmented thrust ratio | Augmented liquid ratio | Maximum augmented thrust ratio | Augmented liquid ratio |
| No afterburning (curve A) | 1.00 | 1.0 | 1.33 | 9.0 |
| Afterburning with JP-3 (curve B) | 1.43 | 4.0 | 1.58 | 7.0 |
| Afterburning with slurry (curve C) | 1.67 | 6.9 | 2.00 | 13.6 |

Without water injection the engine thrust is 17 percent higher with 60-percent-magnesium slurry than with JP-3 fuel. With water injection, the maximum engine thrust with 60-percent-magnesium slurry is 27 percent higher than with JP-3 fuel.

Full-scale experimental results, reported in reference 6, are shown by curve D of figure 10 for an engine using compressor coolant (75 percent water, 25 percent alcohol) injection and afterburning of JP-3 fuel. An augmented thrust ratio of 1.52 was experienced at an augmented liquid ratio of 4, increasing to 1.7 at an augmented liquid ratio of 5.7. Although the general trends are similar, this performance exceeds that of curve B computed from experimental water-injection data and the small-scale afterburner data for JP-3 fuel. There are several reasons for the difference in performance. The engine of curve D employed compressor injection, whereas the engine of curves A, B, and C mainly employed the less effective combustion-chamber injection. The reported combustion efficiency of the afterburner on the engine of curve D exceeded that of the small-scale afterburner with JP-3 fuel.

Effect of afterburning with magnesium slurry upon airplane performance. - Improvements in certain phases of airplane performance may be expected by the use of afterburning with magnesium slurry. The turbojet-engine performance data reported herein for combined water injection and afterburning at sea-level static conditions permit the estimation of reduction in take-off distance due to the use of magnesium slurry.

From augmented thrust ratios shown on curves B and C of figure 10 for a turbojet engine combining afterburning with experimental water-injection performance, the take-off distance of a fighter-type aircraft was computed. It was assumed that the ratio of normal thrust to aircraft weight was 0.33. Take-off characteristics were as follows: drag-lift ratio of 0.15, lift coefficient of 1.0, and wing loading of 60 pounds per square foot. Changes in aircraft weight needed to incorporate various augmentation systems were not considered. The following table presents take-off distance from dry concrete, the ratio

$$\frac{\text{take-off distance with augmented engine}}{\text{take-off distance with unaugmented engine}}$$

and liquid consumption during take-off:

| | Afterburner fuel | Take-off distance (ft) | Fraction of normal take-off distance | Liquid used during take-off[1] (lb) |
|---|---|---|---|---|
| No water injection | None | 3381 | 1.00 | 44 |
| | JP-3 | 2018 | .60 | 113 |
| | Slurry | 1680 | .50 | 136 |
| Water injection | None | 2245 | 0.66 | 267 |
| | JP-3 | 1791 | .53 | 136 |
| | Slurry | 1362 | .40 | 217 |

[1]Based upon 15,000 pound gross weight at take-off.

The replacement of JP-3 by 60-percent-magnesium slurry as an afterburner fuel may result in shortening take-off distance 17 to 24 percent.

2568

## SUMMARY OF RESULTS AND DISCUSSION

The combustion properties of both JP-3 fuel and slurries containing 60 percent magnesium powder with JP-3 fuel were evaluated in a small-scale afterburner in the presence of large quantities of water vapor. From the data thus obtained, the performance of turbojet engines combining water injection and afterburning was estimated. The conclusions are as follows:

1. In the small-scale afterburner, 60-percent-magnesium slurry burned stably to the highest water-air ratio investigated, 0.18, over a wide range of equivalence ratios. Combustion with JP-3 fuel was limited to water-air ratios less than 0.08.

2. The following table shows that total temperatures, combustion efficiencies, and air specific impulses are improved when magnesium slurry rather than JP-3 fuel alone is used in the small-scale afterburner both with and without water vapor. These advantages are at the expense of higher liquid consumption.

| Fuel | Water-air ratio | Afterburner total temperature[1] (°R) | Afterburner combustion efficiency[1] | Air specific impulse[1] (sec) |
|---|---|---|---|---|
| JP-3 | 0 | 3650 | 0.78 | 157 |
| | .07 | 2800 | .56 | 150 |
| Slurry | 0 | 4760 | 0.87 | 177 |
| | .12 | 3720 | .87 | 182 |

[1]Afterburner equivalence ratio, 1.0.

3. The static sea-level performance of a turbojet engine with combined water injection and afterburning of JP-3 fuel or slurry was computed by means of total-temperature data obtained on the small-scale afterburner. Two engines were considered, one making ideal use of injected water and the other utilizing water with experimentally determined effectiveness. The results are listed for an afterburner equivalence ratio of 1.0:

| Type of water injection | Afterburner fuel | No water injection | | Water injection | |
|---|---|---|---|---|---|
| | | Augmented thrust ratio | Augmented liquid ratio | Maximum augmented thrust ratio | Augmented liquid ratio |
| Ideal | JP-3<br>Slurry | 1.47<br>1.75 | 4.0<br>6.9 | 1.81<br>2.15 | 6.8<br>9.8 |
| Experi-mental | JP-3<br>Slurry | 1.43<br>1.67 | 4.0<br>6.9 | 1.58<br>2.00 | 7.0<br>13.6 |

2568

4. The use of magnesium slurry as an afterburner fuel in place of JP-3 fuel may shorten the take-off distance of some aircraft 17 to 24 percent.

Lewis Flight Propulsion Laboratory
National Advisory Committee for Aeronautics
Cleveland, Ohio

## APPENDIX A

## SYMBOLS

The following symbols are used in the report and appendixes:

$A$ area, sq ft

2568 $C_D$ internal drag coefficient of afterburner

$c_{MgO}$ specific heat of magnesium oxide, (Btu/(lb)(mole)(°F)

$c_p$ specific heat at constant pressure, (Btu/(lb)(mole)(°F)

E.R. equivalence ratio of afterburner

$F$ thrust, lb

$f$ liquid-to-air ratio

$f_{b,s}$ stoichiometric fuel-air ratio for afterburner fuel

$g$ acceleration due to gravity, 32.17 ft/sec$^2$

$H$ total sensible enthalpy, Btu/lb mixture

$h$ static sensible enthalpy, Btu/lb mixture

$J$ mechanical equivalent of heat, 778 ft-lb/Btu

$M$ Mach number

$m$ molecular weight

$N$ number of moles

$P$ total pressure, lb/sq ft

$p$ static pressure, lb/sq ft

$Q_i$ heat entering afterburner in form of fuel, Btu/lb mixture

$Q_R$ measured heat loss to afterburner cooling air, Btu/lb mixture

$q$ heating value of fuel, Btu/lb fuel

R universal gas constant, 1545 ft mol/$^{\circ}$R

r weight fraction of magnesium in afterburner fuel

$S_a$ air specific impulse, sec

$S_a^*$ air specific impulse at M = 1, sec

T total temperature, $^{\circ}$R

t static temperature, $^{\circ}$R

V velocity, ft/sec

$V_0$ airplane velocity, ft/sec

W weight flow, lb/sec

$\gamma$ ratio of specific heats

$\Delta P_f$ total pressure loss in an afterburner due to burner and flame-holder drag and inlet diffuser inefficiency, lb/sq ft

$\Delta P_m$ momentum total-pressure loss in an afterburner due to burning, lb/sq ft

$\eta$ efficiency

$\rho$ density of fuel, lb/cu ft

$\varphi(M)$ stream thrust-correction factor to M = 1

Subscripts:

A,B... denotes species of gaseous atoms and molecules present in hot combustion products

a air

au augmented

b afterburner fuel

c afterburner combustion

d afterburner-inlet diffuser

e engine exhaust products

2568

2568

| | |
|---|---|
| g | gaseous phase |
| h | propane |
| j | jet |
| k | afterburner exhaust products |
| n | nozzle |
| t | total |
| u | unaugmented |
| w | water |
| 0 | free stream |
| 1 | compressor inlet |
| 3 | compressor outlet |
| 5 | turbine outlet |
| 6 | afterburner inlet |
| 7 | afterburner outlet |
| 8 | exhaust-nozzle outlet |

## APPENDIX B

## THERMODYNAMIC PROPERTIES OF AFTERBURNER-INLET MIXTURES AND PRODUCTS OF COMBUSTION

2568

In order to reduce the jet-velocity data from the small-scale afterburner to predicted full-scale-engine performance, certain thermodynamic properties of the exhaust products were needed. These properties included: mean molecular weight of gaseous products $m_g$; ratio of specific heats $\gamma$; and sensible enthalpy $h$. A knowledge of combustion-product composition at high temperatures, including dissociation effects, was necessary first. At assigned elevated temperatures the equilibrium composition of the combustion products at an equivalence ratio of 1.0 was found by a method adapted from reference 13. A pressure of 2 atmospheres was arbitrarily assigned to the computations. It was assumed that there were no products of incomplete combustion present. The compositions of the fuel-air mixtures before combustion were those defined by the curves of figure 5.

From the product compositions thus determined and tables of thermodynamic properties of the constituents (reference 14) mean molecular weight of gaseous products was computed from the expression

$$m_g = \frac{N_A m_A + N_B m_B + \ldots}{N_A + N_B} \tag{B1}$$

The value of specific-heat ratio $\gamma$ was defined as

$$\gamma = \frac{N_A c_{p,A} + N_B c_{p,B} + \ldots + N_{MgO} c_{MgO}}{N_A c_{p,A} + N_B c_{p,B} + \ldots + N_{MgO} c_{MgO} - 1.9876(N_t - N_{MgO})} \tag{B2}$$

The sensible enthalpy of products of afterburning was defined as

$$h = \frac{N_A h_A m_A + N_B h_B m_B + \ldots + N_{MgO} h_{MgO} m_{MgO}}{N_A m_A + N_B m_B + \ldots + N_{MgO} m_{MgO}} \tag{B3}$$

The sensible enthalpy was also computed for afterburner-inlet mixtures consisting of liquid fuel at 537° R and products of propane combustion with water vapor at 1660° R.

These thermodynamic properties are presented in figures 11 and 12 at an equivalence ratio of 1.0 for JP-3 fuel and 60-percent-magnesium slurry.

2568

## APPENDIX C

## REDUCTION OF DATA FROM 6-INCH SMALL-SCALE AFTERBURNER

Afterburner equivalence ratio. - The afterburner equivalence ratio E.R. was found as follows:

$$\text{E.R.} = \frac{f_b}{f_{b,s}}\left(1 - \frac{f_h}{0.0640}\right) \tag{C1}$$

where $f_{b,s}$ is 0.1305 for 60-percent-magnesium slurry or 0.0675 for JP-3 fuel.

Velocity at the afterburner exit nozzle. - The velocity was computed from the expression

$$V_8 = \frac{g\,F_j}{W_a + W_h + W_b + W_w} = \frac{g\,F_j}{W_t} \tag{C2}$$

One-dimensional flow with velocity and temperature equilibrium of both gaseous and solid products was assumed.

Air specific impulse at M = 1. - Air specific impulse at Mach number 1 is defined as

$$S_a^* = \frac{1}{W_a}\left(p_8 A_8 + \frac{W_t V_8}{g}\right)\varphi(M_8) \tag{C3}$$

where

$$\varphi(M_8) = \frac{M_8\left(\sqrt{2(\gamma+1)}\right)\left[1 + \frac{1}{2}(\gamma-1)M_8^2\right]^{\frac{1}{2}}}{1 + \gamma M_8^2}$$

The function $\varphi(M_8)$ reduces $S_a$ at any Mach number to $S_a^*$ at $M = 1$. The stream thrust-correction factor $\varphi(M_8)$ may be found for any $M_8$ and $\gamma$ as the reciprocal of $F/F^*$ in tables 30 through 35 of reference 15. For the data reported herein a ratio of specific heats $\gamma$ of 1.3 has been arbitrarily used in determining $\varphi(M_8)$.

Afterburner total temperature. - The weight of gaseous products for the slurry runs was

$$W_g = W_a + W_h + W_b + W_w - \frac{40.32}{24.32} r\, W_b \qquad \text{(C4)}$$

2568

and for the JP-3 fuel runs

$$W_g = W_a + W_h + W_b + W_w = W_t$$

The exhaust-nozzle-jet velocities at an equivalence ratio of 1.0 were found by a graphical interpolation among the data shown in table III. Static temperature was then determined as

$$t_8 = \frac{p_8 A_8 V_8 m_g}{R\, W_g} \qquad \text{(C5)}$$

The corresponding static enthalpy was read from figure 11(b) or 12(b). The total enthalpy per pound of exhaust products was then

$$H_8 = h_8 + \frac{V_8^2}{2gJ} + Q_R \qquad \text{(C6)}$$

The total enthalpy was thus corrected for the measured heat loss $Q_R$ to the afterburner cooling air. By the use of $H_8$ and figure 11(b) or 12(b) total temperature was found.

Afterburner combustion efficiency. - Afterburner combustion efficiency is defined as

$$\eta_c = \frac{\Delta H\Big]_6^8}{Q_i} = \frac{W_t(H_8 - H_6)}{q_b W_b} \qquad \text{(C7)}$$

where $q_b$ = 13,966 Btu/lb of 60-percent-magnesium slurry or 18,800 Btu/lb of JP-3 fuel. The afterburner-inlet-mixture enthalpy $H_6$ was found from figure 11(a) or 12(a).

2568

## APPENDIX D

## COMPUTATION OF THRUST AUGMENTATION FOR TURBOJET ENGINES

The ratio of augmented to normal net thrust is

$$\frac{F_{au}}{F_u} = \frac{F_{au,j} - W_{a,au}\, V_0}{F_{u,j} - W_{a,u}\, V_0} \tag{D1}$$

For the analysis presented herein, the airplane speed $V_0$ is zero or nearly zero; hence, the jet thrust ratio $F_{au,j}/F_{u,j}$ is equal to the net thrust ratio $F_{au}/F_u$.

Thrust of engines with water injection alone. - The jet thrust of the engine for an unchoked exhaust nozzle is (reference 16)

$$F_j = \frac{W_t}{g}\sqrt{2g\eta_n \frac{\gamma_e}{\gamma_e - 1} \frac{RT_5}{m_g}\left[1 - \left(\frac{p_0}{P_5}\right)^{\frac{\gamma_e - 1}{\gamma_e}}\right]} \tag{D2}$$

and for a choked exhaust nozzle is

$$F_j = \frac{W_t}{g}\sqrt{2g \frac{\gamma_e}{\gamma_e + 1} \frac{RT_5}{m_g}\left[1 + \frac{1}{\gamma_e}\left(1 - \frac{p_0}{p_8}\right)\right]} \tag{D3}$$

where

$$\frac{p_0}{p_8} = \frac{1}{\frac{P_5}{p_0}\left[1 - \left(\frac{\gamma_e - 1}{\gamma_e + 1}\right)\frac{1}{\eta_n}\right]^{\frac{\gamma_e}{\gamma_e - 1}}} \tag{D4}$$

Both equations (D2) and (D3) require that the ratio $P_5/p_0$ at the turbine outlet be known. For the engine without afterburner, no drag or diffusion pressure losses were assumed between the turbine discharge and the exhaust-nozzle opening. Diagrams of both engine types are shown in figure 13.

The variation of $P_5/p_0$ with water-air ratio for the engine employing ideal water injection and for the engine making experimentally determined use of water injection is shown in figure 14. For the theoretical engine, $P_5/p_0$ was computed by the method of reference 16, with the following assumptions: The air inducted into the compressor had a relative humidity of 0.50 and NACA standard sea-level pressure and temperature; the compressor adiabatic efficiency was $0.8 - \left[\Delta X\right]_1^3$, where $\left[\Delta X\right]_1^3$ was the quantity of water vaporized in the compressor; the work output per pound of mixture was 85.3 Btu; total pressure loss within the combustion chambers was 3 percent; turbine adiabatic efficiency was 85 percent; and turbine-inlet temperature was 2000° R. 2568

The engine with experimental water-injection performance operated at a turbine-outlet temperature $T_5$ of 1725° R; the engine with ideal water injection, at about 1700° R. Normal compressor pressure ratio for both engines was 4.6.

<u>Thrust of engine with combined water injection and afterburning</u>. - The jet thrust of the engine for the unchoked exhaust nozzle was

$$F_j = \frac{W_t}{g}\sqrt{2g\eta_n \frac{\gamma_k}{\gamma_k - 1} \frac{RT_8}{m_g} \left[1 - \left(\frac{p_0}{P_7}\right)^{\frac{\gamma_k - 1}{\gamma_k}}\right]} \tag{D5}$$

For the choked nozzle, with or without solid exhaust products

$$F_j = \frac{W_t}{g}\sqrt{2g \frac{\gamma_k}{\gamma_k + 1} \frac{RT_8}{m_g}} \left[1 + \frac{1}{\gamma_k}\left(1 - \frac{p_0}{p_8}\right)\left(1 - \frac{W_{MgO}}{W_t}\right)\right] \tag{D6}$$

where

$$\frac{p_0}{p_8} = \frac{1}{\frac{P_7}{p_0}\left[1 - \left(\frac{\gamma_k - 1}{\gamma_k + 1}\right)\frac{1}{\eta_n}\right]^{\frac{\gamma_k}{\gamma_k - 1}}} \tag{D7}$$

The same characteristics were assumed for the afterburner of both engines. These characteristics were as follows: The afterburner-inlet velocity was 400 feet per second; the adiabatic efficiency of the diffusion process in the afterburner-inlet diffuser was 0.8; the afterburner drag coefficient was 1.0; and the nozzle adiabatic efficiency was 0.95.

Afterburner total temperatures used were those determined for the small-scale afterburner as shown in figure 7. The afterburner-inlet temperatures were lower in the small-scale afterburner (1660° R) than in the full-scale engines (1700° and 1725° R). The error introduced by the use of these temperatures without correction in analyzing the performance of the full-scale engine was small, however.

The pressure ratio $P_7/p_0$ at the afterburner exhaust nozzle was less than the ratio $P_5/p_0$ at the turbine outlet, shown in figure 14, because of losses. These losses depended upon afterburner temperature rise $T_8/T_5$, drag $C_D$, inlet diffuser efficiency $\eta_d$, and inlet velocity factor $V_5\sqrt{1600/T_5}$. They have been separated into two groups, $\Delta P_f/P_5$ and $\Delta P_m/P_6$, and were found by the use of figure 15, redrawn from reference 17. The pressure ratio $P_7/p_0$ across the afterburner exhaust nozzle was then

$$\frac{P_7}{p_0} \cong \frac{P_5}{p_0}\left[1 - \left(\frac{\Delta P_f}{P_5} + \frac{\Delta P_m}{P_6}\right)\right] \qquad \text{(D8)}$$

## REFERENCES


1. Olson, Walter T., and Gibbons, Louis C.: Status of Combustion Research on High-Energy Fuels for Ram-Jets. NACA RM E51D23, 1951.

2. Tower, Leonard K., and Branstetter, J. Robert: Combustion Performance Evaluation of Magnesium-Hydrocarbon Slurry Blends in a Simulated Tail-Pipe Burner. NACA RM E51C26, 1951.

3. Gibbs, James B., and Cook, Preston N., Jr.: Preparation and Physical Properties of Metal Slurry Fuels. NACA RM E52A23, 1952.

4. Lord, Albert M.: An Experimental Investigation of the Combustion Properties of a Hydrocarbon Fuel and Several Magnesium and Boron Slurries. NACA RM E52B01, 1952.

5. Hall, Eldon W., and Wilcox, E. Clinton: Theoretical Comparison of Several Methods of Thrust Augmentation for Turbojet Engines. NACA Rep. 992, 1950. (Supersedes NACA RM E8H11.)

6. Useller, James W., and Povolny, John H.: Experimental Investigation of Turbojet-Engine Thrust Augmentation by Combined Compressor Coolant Injection and Tail-Pipe Burning. NACA RM E51H16, 1951.

7. Jacobson, C. A.: Encyclopedia of Chemical Reactions. Vol. IV. Reinhold Pub. Corp. (New York), 1951.

8. Perry, John H.: Chemical Engineers Handbook. McGraw-Hill Book Co., Inc., 3d ed., 1950.

9. Terem, Holdun N.: Studies of Dry Corrosion. Oxidation of Magnesium. Chem. Abs., vol. 42, no. 20, Oct. 20, 1948. Abs. from Rev. faculte sci. univ. Istanbul 13A, 1948, pp. 147-159.

10. Rudnick, Philip: Momentum Relations in Propulsive Ducts. Jour. Aero. Sci., vol. 14, no. 9, Sept. 1947, pp. 540-544.

11. Boman, Davis S., and Mallett, William E.: Investigation of Thrust 2568
Augmentation Using Water-Alcohol Injection on a 5200-Pound-Thrust Axial-Flow-Type Turbojet Engine at Static Sea-Level Conditions. NACA RM E52G30, 1952.

12. Povolny, John H., Useller, James W., and Chelko, Louis J.: Experimental Investigation of Thrust Augmentation of 4000-Pound-Thrust Axial-Flow-Type Turbojet Engine by Interstage Injection of Water Alcohol Mixture in Compressor. NACA RM E9K30, 1950.

13. Huff, Vearl N., and Morrell, Virginia E.: General Method for Computation of Equilibrium Composition and Temperature of Chemical Reactions. NACA TN 2113, 1950.

14. Huff, Vearl N., and Gordon, Sanford: Tables of Thermodynamic Functions for Analysis of Aircraft-Propulsion Systems. NACA TN 2161, 1950.

15. Keenan, Joseph H., and Kaye, Joseph: Gas Tables - Thermodynamic Properties of Air, Products of Combustion and Component Gases, Compressible Flow Functions. John Wiley and Sons, Inc., 1948.

16. Wilcox, E. Clinton, and Trout, Arthur M.: Analysis of Thrust Augmentation of Turbojet Engines by Water-Injection at Compressor Inlet Including Charts for Calculating Compression Processes with Water Injection. NACA Rep. 1006, 1951. (Supersedes NACA TN's 2104 and 2105.)

17. Bohanon, H. R., and Wilcox, E. C.: Theoretical Investigation of Thrust Augmentation of Turbojet Engines by Tail-Pipe Burning. NACA RM E6L02, 1947.

2568

TABLE I - SPECIFICATIONS AND ANALYSIS OF REFERENCE FUEL

| | Specifications MIL-F-5624 | Analysis MIL-F-5624 NACA 51-21 |
|---|---|---|
| A.S.T.M. distillation D86-46, °F | | |
| Initial boiling point | ------------- | 112 |
| Percent evaporated | | |
| 5 | ------------- | 141 |
| 10 | ------------- | 164 |
| 20 | ------------- | 216 |
| 30 | ------------- | 266 |
| 40 | ------------- | 304 |
| 50 | ------------- | 340 |
| 60 | ------------- | 374 |
| 70 | ------------- | 406 |
| 80 | ------------- | 433 |
| 90 | 400 (min.) | 464 |
| Final boiling point | 600 (max.) | 522 |
| Residue, (percent) | 1.5 (max.) | 1.2 |
| Loss, (percent) | 1.5 (max.) | 0.8 |
| Aromatics, (percent by volume) A.S.T.M. D875-46 T | 25 (max.) | <5 |
| Specific gravity | 0.728 (min.) | 0.753 |
| Reid vapor pressure, (lb/sq in.) | 5-7 | 4.8 |
| Hydrogen-carbon ratio | ------------- | 0.174 |
| Net heat of combustion, (Btu/lb) | 18,400 (min.) | 18,841 |

TABLE II - CHARACTERISTICS OF MAGNESIUM POWDER

| Type of magnesium powder | Uncombined magnesium (percent)[a] | Particle size distribution | |
|---|---|---|---|
| | | Total number of particles (percent) | Particle size (microns) |
| Atomized | 99 | 0-1/2 | 25-40 |
| | | 1-2 | 6-25 |
| | | 3-5 | 3-6 |
| | | Balance | 0-3 |

[a]Manufacturer's estimate.

[redacted]

TABLE III - PERFORMANCE DATA FOR SMALL-SCALE AFTERBURNER

[Exhaust nozzle area, 17.25 sq in.]

| Magnesium in afterburner fuel (percent) | Air flow (lb/sec) | Propane flow (lb/sec) | Primary combustor fuel-air ratio | Afterburner-inlet temperature (°F) | Afterburner-inlet total pressure (lb/sq in. abs) | Afterburner fuel flow (lb/sec) | Afterburner equivalence ratio | Water-air ratio | Target thrust (lb) | Target static pressure (lb/sq in. abs) | Exhaust-nozzle jet velocity (ft/sec) | Approximate exhaust Mach number | Stream thrust-correction factor φ(M) | Air specific impulse $S_a^*$ (sec) | Fuel specific impulse (sec) | Heat rejected through burner wall (Btu/lb mixture) | Comments |
|---|---|---|---|---|---|---|---|---|---|---|---|---|---|---|---|---|---|
| 60 | 2.47 | 0.0397 | 0.0161 | 1200 | 20.6 | 0.142 | 0.59 | 0 | 155 | 14.4 | 1878 | 0.67 | 0.958 | 153 | 2079 | 20 | |
| | 2.47 | .0555 | .0224 | 1200 | 21.2 | .157 | .65 | .068 | 173 | 14.4 | 1965 | .71 | .956 | 163 | 1116 | 26 | |
| | 2.46 | .0626 | .0254 | 1190 | 21.2 | .127 | .80 | .106 | 171 | 14.3 | 1882 | .71 | .954 | 162 | 885 | 26 | |
| | 2.48 | .0731 | .0298 | 1190 | 20.1 | .137 | .77 | .154 | 179 | 14.4 | 1889 | .73 | .960 | 167 | 698 | 24 | |
| | 2.45 | .0725 | .0299 | 1190 | 21.1 | .130 | .77 | .156 | 176 | 14.4 | 1887 | .72 | .958 | 166 | 701 | 25 | |
| | 2.48 | .0546 | .0220 | 1200 | 21.8 | .164 | .77 | 0.067 | 183 | 14.4 | 2056 | .73 | .962 | 167 | 1077 | 27 | |
| | 2.52 | .0432 | .0171 | 1225 | 21.1 | .168 | .86 | 0 | 170 | 14.4 | 2017 | .71 | .952 | 158 | 1981 | 28 | |
| | 2.44 | .0406 | .0166 | 1200 | 21.1 | .181 | .88 | 0 | 164 | 14.4 | 2000 | .69 | .948 | 160 | 1939 | 27 | |
| | 2.48 | .0407 | .0164 | 1200 | 22.0 | .184 | .80 | 0 | 187 | 14.4 | 2210 | .73 | .962 | 169 | 1728 | 28 | |
| | 2.41 | .0804 | .0250 | 1200 | 22.6 | .200 | 1.04 | .102 | 207 | 14.4 | 2288 | .77 | .975 | 184 | 877 | 29 | |
| | 2.45 | .0725 | .0297 | 1220 | 22.2 | .195 | 1.14 | .153 | 205 | 14.4 | 2123 | .77 | .973 | 181 | 688 | 28 | |
| | 2.43 | .0721 | .0297 | 1255 | 22.2 | .193 | 1.13 | .153 | 199 | 14.4 | 2093 | .76 | .970 | 179 | 684 | 28 | |
| | 2.44 | .0393 | .0161 | 1215 | 19.4 | .087 | .37 | | 129 | 14.4 | 1618 | .62 | .912 | 142 | 2725 | 26 | |
| | 2.45 | .0498 | .0204 | 1190 | 20.0 | .099 | .46 | .054 | 147 | 14.4 | 1751 | .66 | .933 | 152 | 1324 | 20 | |
| | 2.42 | .0545 | .0225 | 1205 | 19.8 | .099 | .46 | .087 | 149 | 14.4 | 1748 | .67 | .955 | 153 | 1172 | 20 | |
| | 2.47 | .0598 | .0242 | 1185 | 19.4 | .098 | .49 | .098 | 134 | 14.4 | 1505 | .63 | .920 | 143 | 880 | 18 | |
| | 2.42 | .0774 | .0320 | 1115 | 18.8 | .096 | .61 | .178 | 123 | 14.4 | 1314 | .61 | .907 | 139 | 559 | 17 | |
| | 2.47 | .0782 | .0317 | 1100 | 19.4 | .117 | .72 | .174 | 127 | 14.4 | 1329 | .62 | .911 | 139 | 548 | 15 | |
| | 2.48 | .0410 | .0165 | 1200 | 20.2 | .116 | .49 | 0 | 149 | 14.4 | 1817 | .66 | .934 | 149 | 2533 | 22 | |
| | 2.41 | .0506 | .0241 | 1225 | 20.4 | .120 | .57 | .054 | 154 | 14.4 | 1827 | .67 | .938 | 157 | 1258 | 22 | |
| | 2.52 | .0622 | .0247 | 1200 | 21.1 | .116 | .58 | .092 | 172 | 14.4 | 1891 | .71 | .956 | 180 | 978 | 21 | |
| | 2.48 | .0599 | .0241 | 1210 | 21.0 | .118 | .58 | .094 | 171 | 14.4 | 1909 | .71 | .966 | 182 | 978 | 25 | |
| | 2.48 | .0407 | .0165 | 1208 | 21.2 | .173 | .72 | 0 | 189 | 14.4 | 2018 | .70 | .949 | 160 | 1857 | 28 | |
| 60 | 2.52 | .0393 | .0157 | 1105 | 24.3 | .360 | 1.44 | 0 | 227 | 15.0 | 2635[a] | .79 | .974 | 188 | 470 | 19 | |
| 0 | 2.46 | .0387 | .0162 | 1200 | 18.4 | .055 | .44 | 0 | 110 | 14.4 | 1390 | .58 | .890 | 130 | 3367 | 19 | |
| | 2.46 | .0434 | .0176 | 1200 | 18.6 | .055 | .46 | .021 | 114 | 14.4 | 1404 | .59 | .897 | 132 | 2146 | 19 | |
| | 2.47 | .0434 | .0176 | 1180 | ---- | .056 | .46 | .025 | --- | ---- | ---- | ---- | ----- | --- | ---- | -- | Blow-out |
| | 2.47 | .0390 | .0158 | 1190 | 18.8 | .065 | .51 | 0 | 121 | 14.4 | 1517 | .61 | .908 | 136 | 3257 | 19 | |
| | | | | | | | | | | | 1 | .62 | | | | | |
| | 2.48 | .0393 | .0157 | 1186 | 18.9 | .064 | .54 | .033 | 123 | 14.4 | 1493 | .62 | .912 | 138 | 1778 | 20 | |
| | 2.46 | .0397 | .0162 | 1210 | 19.1 | .063 | .57 | .059 | 128 | 14.4 | 1517 | .63 | .918 | 141 | 1328 | 20 | |
| | 2.46 | .0434 | .0176 | 1215 | ---- | .063 | .58 | .068 | --- | ---- | ---- | ---- | ----- | --- | ---- | -- | Blow-out |
| | 2.47 | .0434 | .0176 | 1210 | 19.5 | .081 | .66 | 0 | 135 | 14.4 | 1698 | .65 | .927 | 146 | 2925 | 22 | |
| | 2.47 | .0390 | .0158 | 1200 | 19.6 | .081 | .69 | .035 | 138 | 14.4 | 1677 | .65 | .930 | 147 | 1708 | 23 | |
| | 2.47 | .0509 | .0208 | 1205 | 19.8 | .081 | .72 | .054 | 144 | 14.4 | 1896 | .67 | .936 | 149 | 1384 | 22 | |
| | 2.43 | .0538 | .0222 | 1195 | 19.1 | .082 | .76 | .074 | 128 | 14.5 | 1500 | .63 | .917 | 142 | 1098 | 21 | |
| | 2.45 | .0553 | .0226 | 1165 | 18.5 | .083 | .77 | .078 | 118 | 14.5 | 1364 | .60 | .902 | 135 | 1007 | 18 | Blow-out near end of run |
| | 2.44 | .0392 | .0161 | 1200 | 20.1 | .110 | .89 | 0 | 151 | 14.5 | 1878 | .68 | .942 | 155 | 2527 | 24 | |
| | 2.44 | .0452 | .0186 | 1210 | 20.3 | .109 | .93 | .029 | 154 | 14.5 | 1868 | .69 | .946 | 157 | 1703 | 26 | |
| | 2.46 | .0518 | .0211 | 1200 | 20.1 | .109 | .98 | .064 | 147 | 14.5 | 1707 | .67 | .938 | 152 | 1175 | 25 | |
| | 2.45 | .0541 | .0221 | 1200 | 18.9 | .111 | 1.02 | .074 | 125 | 14.5 | 1442 | .62 | .913 | 139 | 988 | 22 | |
| | 2.48 | .0562 | .0227 | 1195 | 16.8 | .111 | 1.05 | .080 | 114 | 14.5 | 1298 | .59 | .897 | 132 | 894 | 19 | Blow-out near end of run |
| | 2.45 | .0402 | .0164 | 1210 | 20.5 | .146 | 1.19 | 0 | 168 | 14.5 | 1928 | .70 | .949 | 158 | 2081 | 28 | |
| | 2.48 | .0451 | .0186 | 1190 | 20.5 | .141 | 1.18 | .037 | 163 | 14.5 | 1897 | .71 | .952 | 159 | 1404 | 27 | |
| | 2.45 | .0477 | .0195 | 1165 | ---- | .143 | 1.24 | .047 | --- | 14.5 | ---- | ---- | ----- | --- | ---- | -- | Blow-out |
| | 2.46 | .0598 | .0161 | 1200 | 20.5 | .162 | 1.30 | 0 | 158 | 14.5 | 1911 | .70 | .949 | 157 | 1925 | 26 | |
| | 2.42 | .0429 | .0177 | 1200 | 20.2 | .163 | 1.38 | .027 | 155 | 14.5 | 1631 | .69 | .944 | 157 | 1400 | 26 | |

[a]Corrected to target static pressure of 14.4 lb/sq in. abs.

NACA

[redacted]

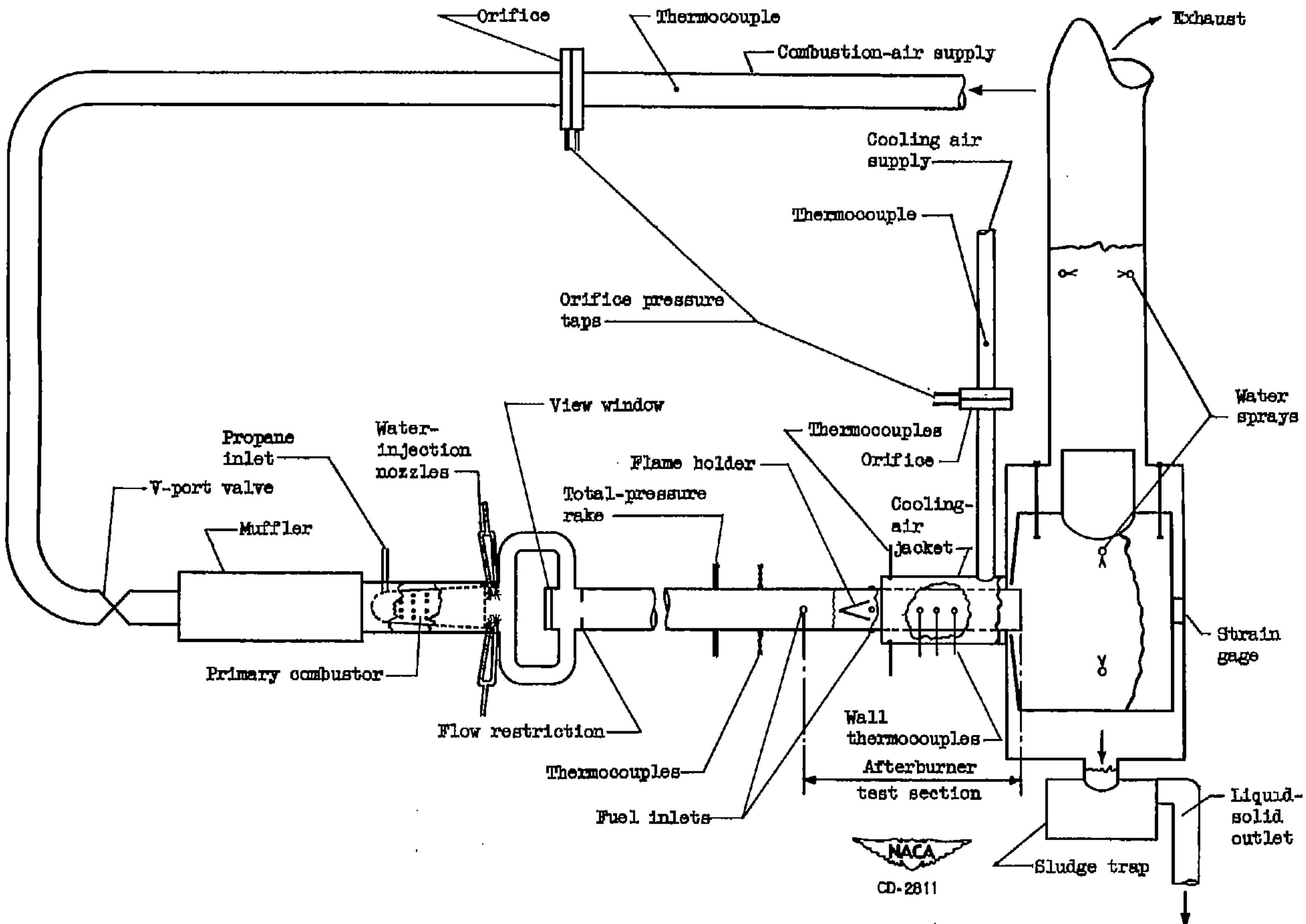


Figure 1. - Diagrammatic sketch of afterburner installation.

2568

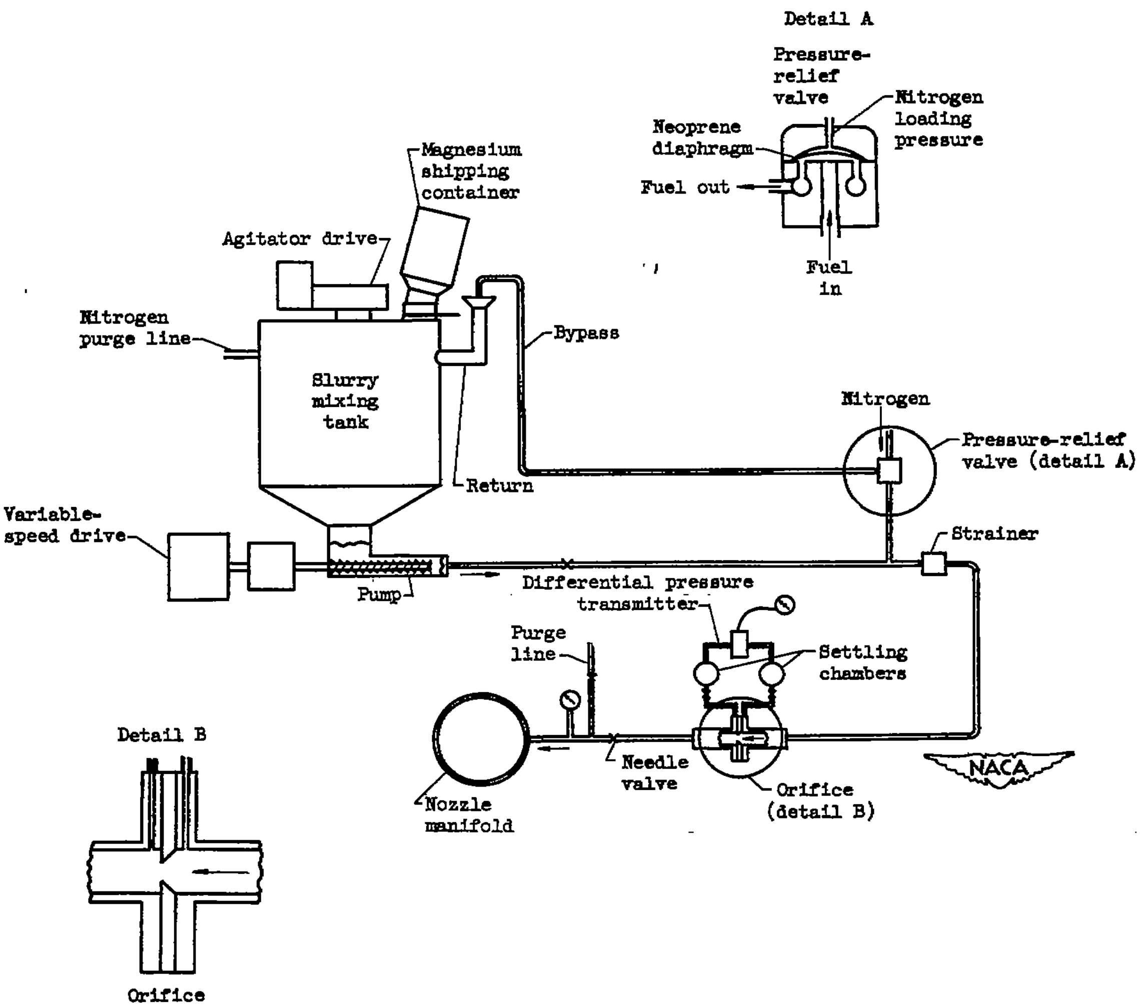


Figure 2. - Diagrammatic sketch of afterburner fuel system.

2568

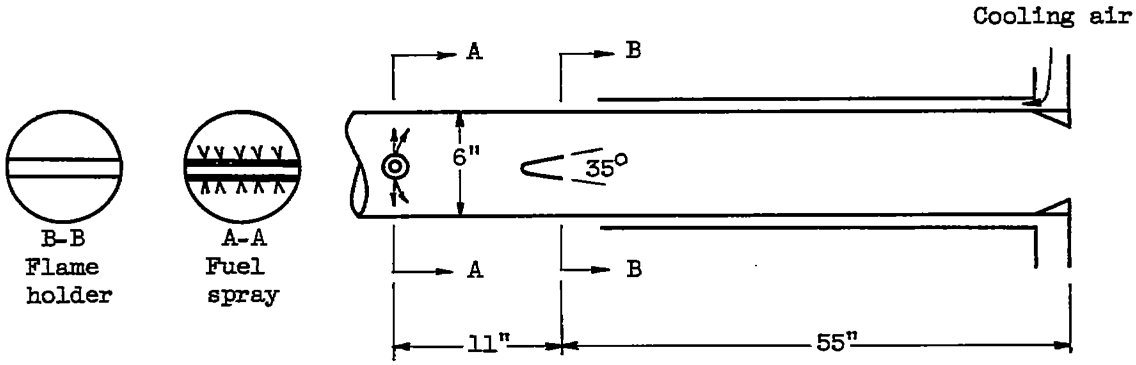


(a) Afterburner configuration. Flame-holder blocked area, 31 percent.

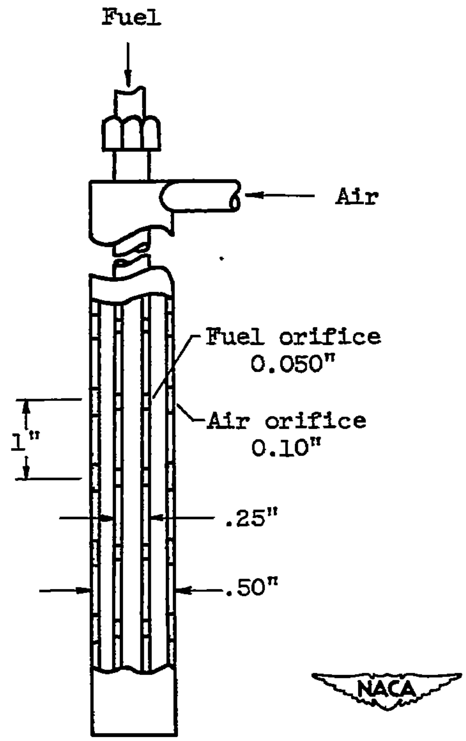


(b) Air-atomizing spray bar.

Figure 3. - Diagrammatic sketch of afterburner configuration and fuel spray used with JP-3 fuel.

2568

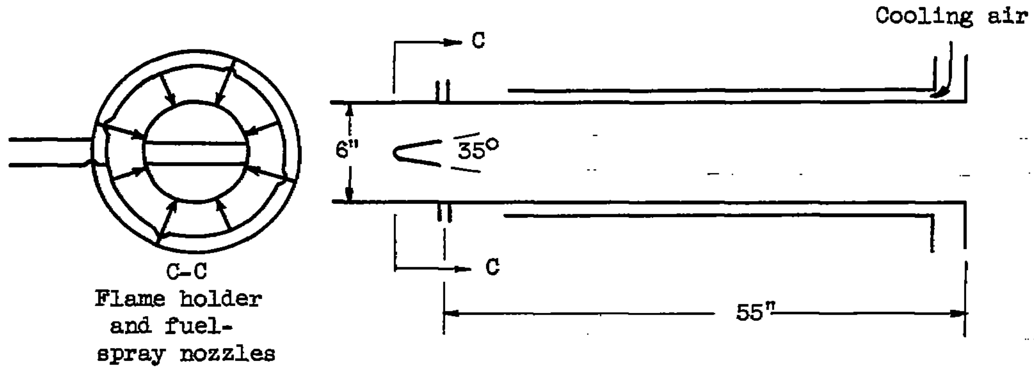


(a) Afterburner configuration. Flame-holder blocked area, 31 percent.

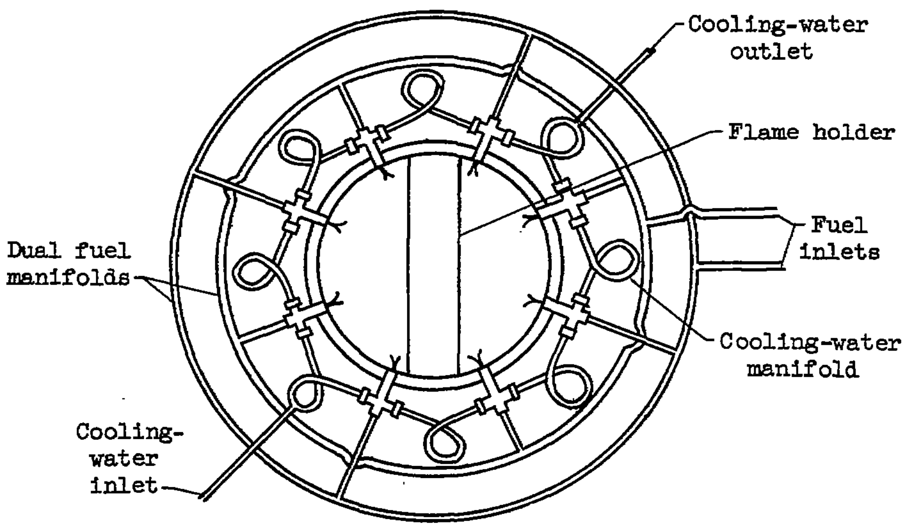


(b) Wall injection nozzle manifold.

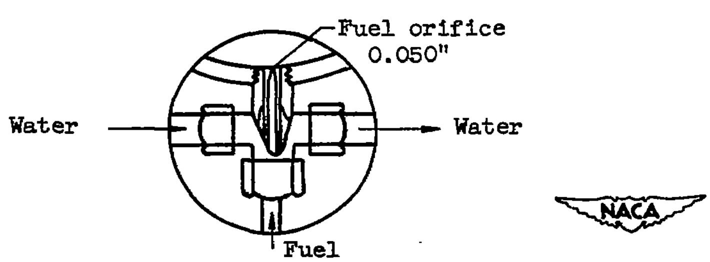


(c) Water-cooled wall injection nozzle.

Figure 4. - Diagrammatic sketch of afterburner configuration, nozzle manifold, and fuel-spray nozzle used with 60-percent atomized-magnesium slurries.

2568

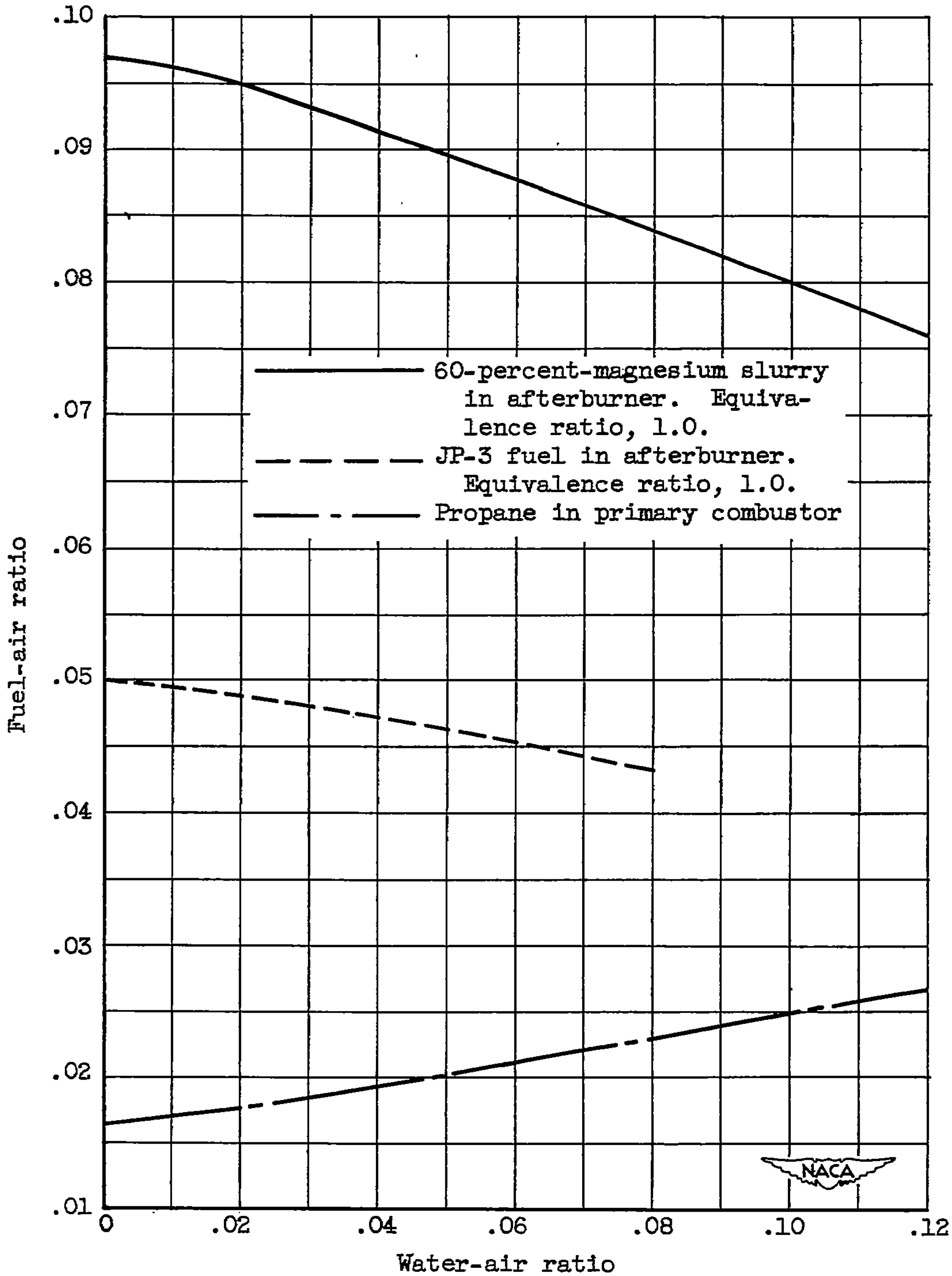


Figure 5. - Variation of propane-air ratio and small-scale-afterburner fuel-air ratio with water-air ratio.

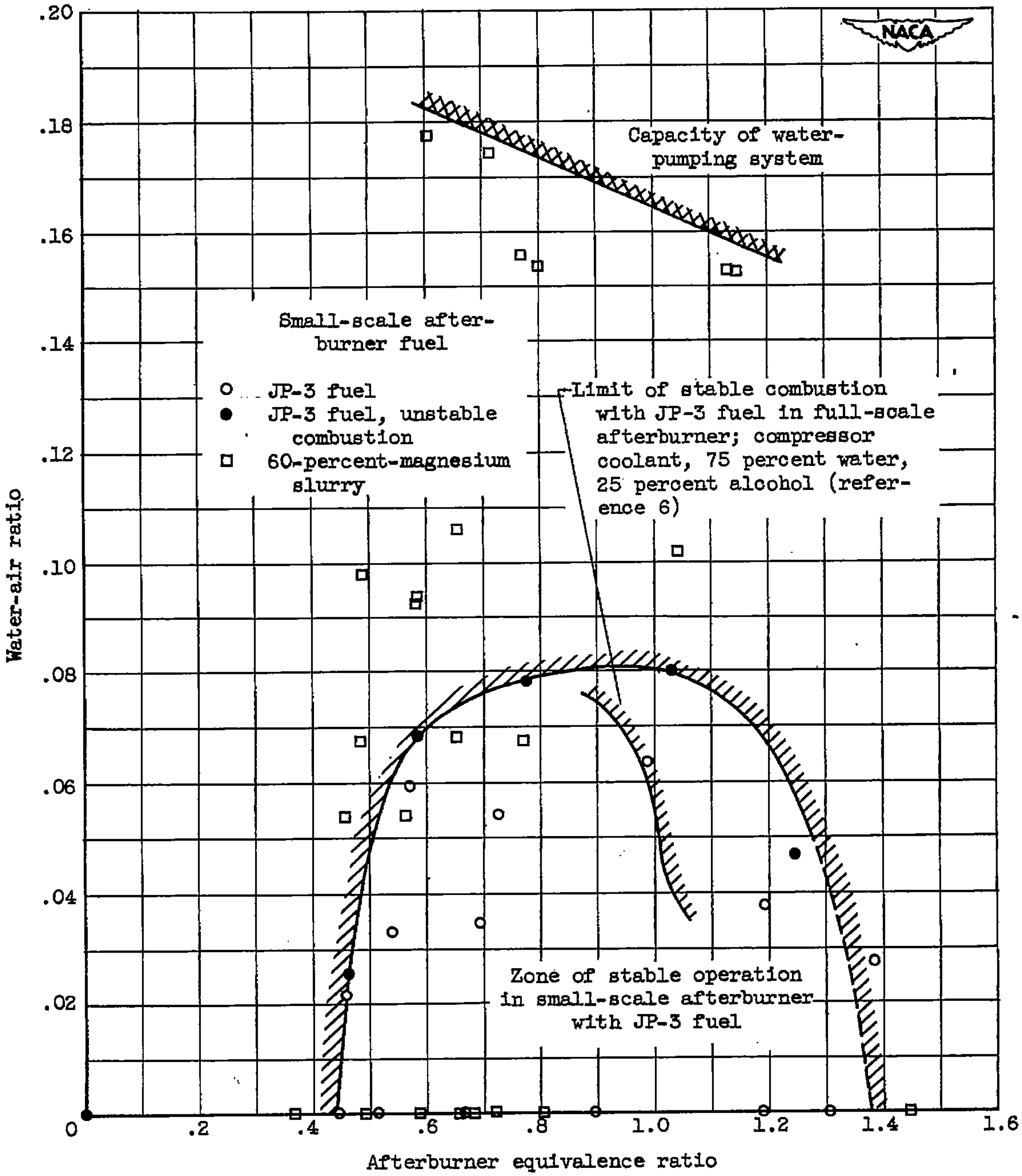


Figure 6. - Range of water-air ratios and afterburner equivalence ratios investigated in small-scale afterburner with JP-3 fuel and 60-percent-magnesium slurry. Afterburner-inlet velocity, 300 to 450 feet per second; afterburner pressure, 16 to 24 pounds per square inch.

2568

2568

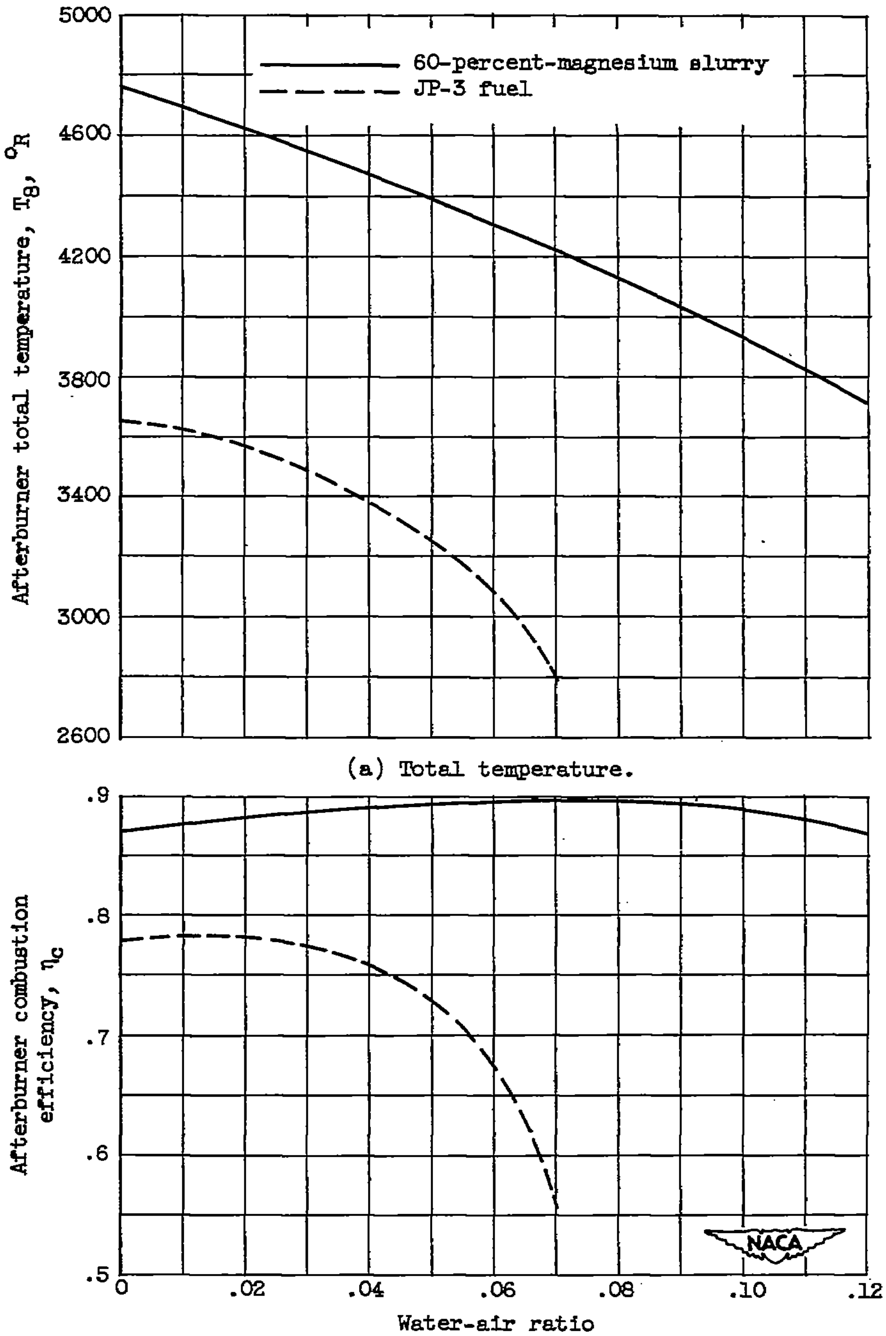


(a) Total temperature.

(b) Combustion efficiency.

Figure 7. - Effect of water-air ratio on small-scale afterburner total temperature and combustion efficiency for JP-3 fuel and 60-percent-magnesium slurry. Afterburner equivalence ratio, 1.0; afterburner inlet velocity, 300 to 450 feet per second; afterburner pressure, 16 to 24 pounds per square inch.

2568

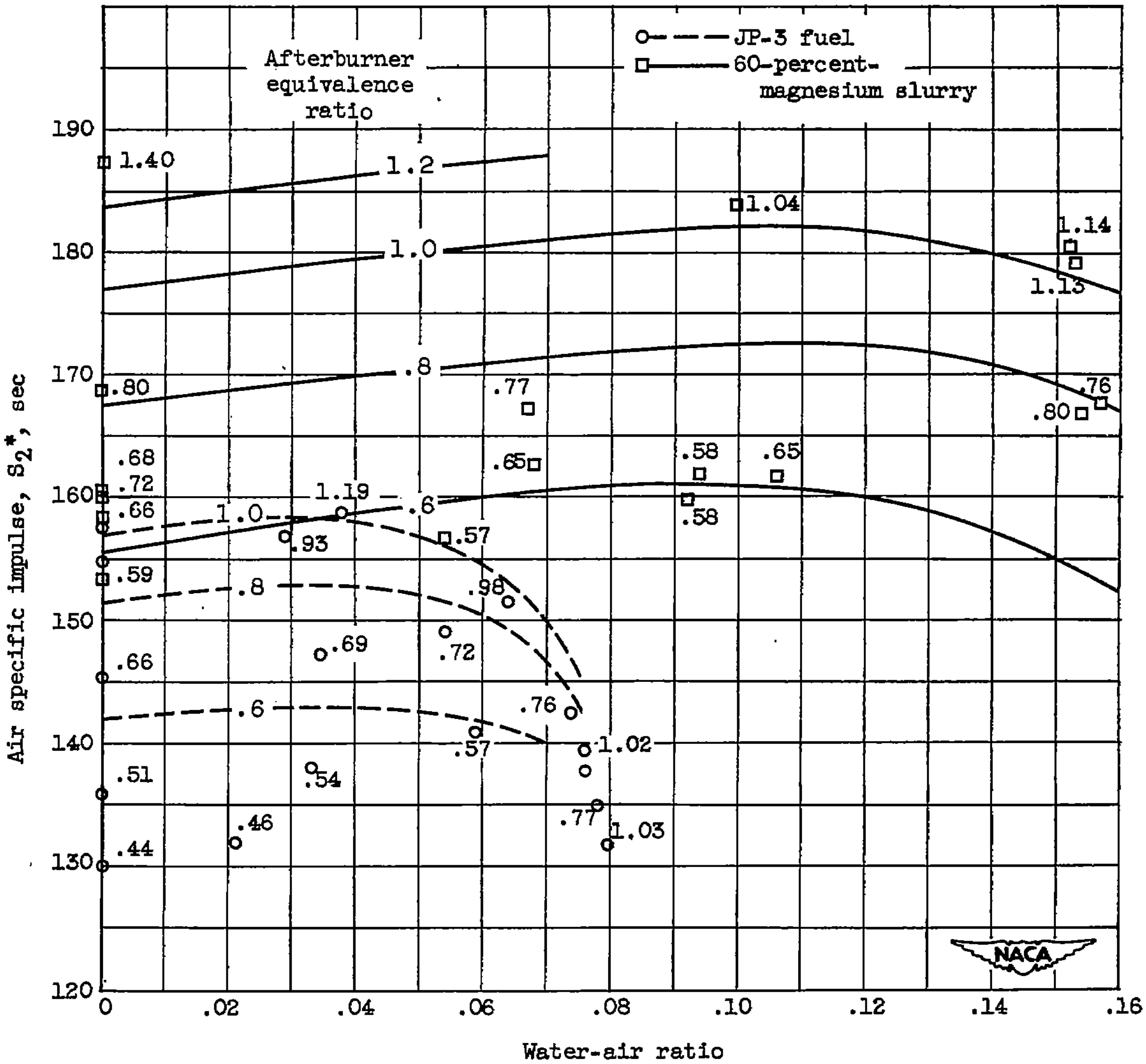


Figure 8. - Variation of air specific impulse with water-air ratio and equivalence ratio in small-scale afterburner using JP-3 fuel and 60-percent-magnesium slurry. Afterburner-inlet velocity, 300 to 450 feet per second; afterburner pressure, 16 to 24 pounds per square inch. Lines represent constant equivalence ratios.

2568

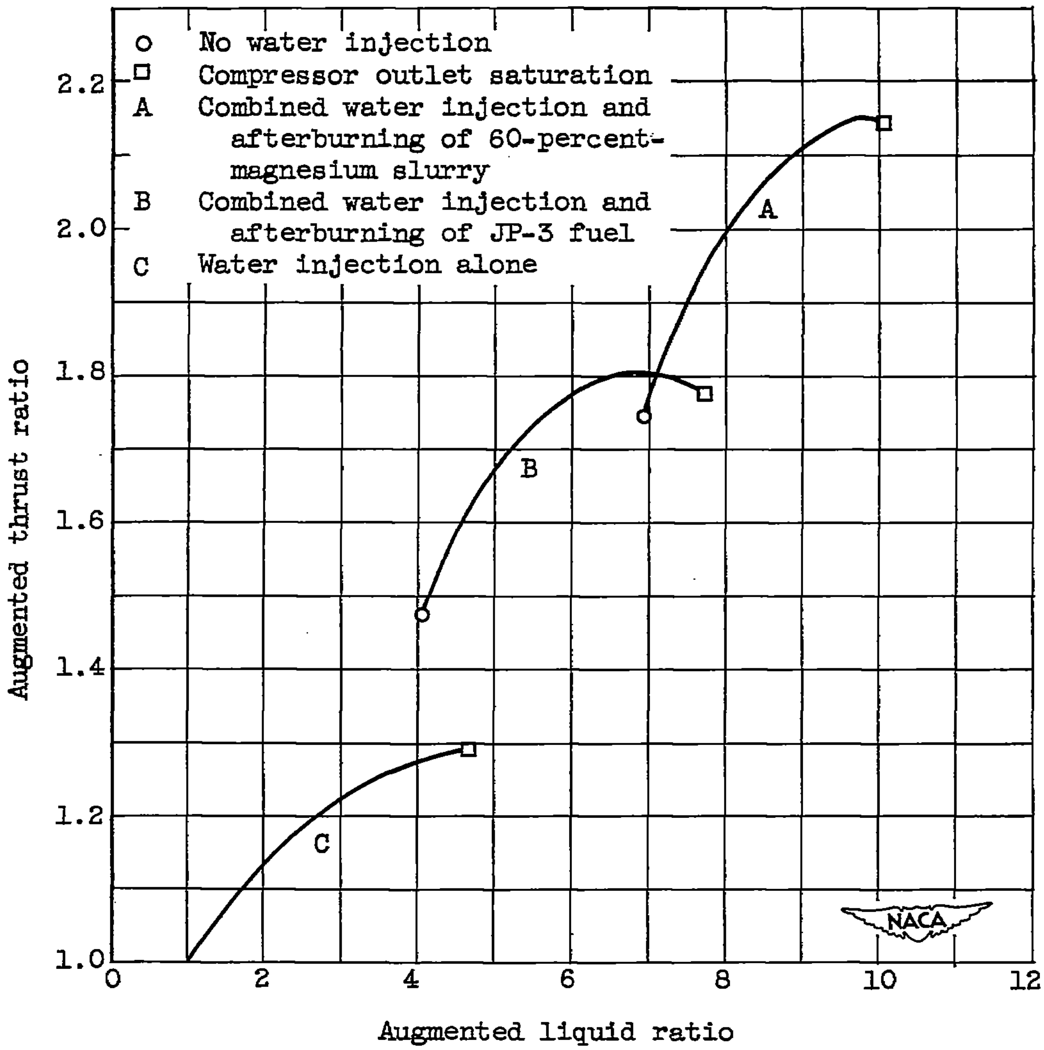


Figure 9. - Static sea-level thrust augmentation of turbojet engine combining afterburning with ideal water-injection performance. Afterburner equivalence ratio, 1.0.

2568

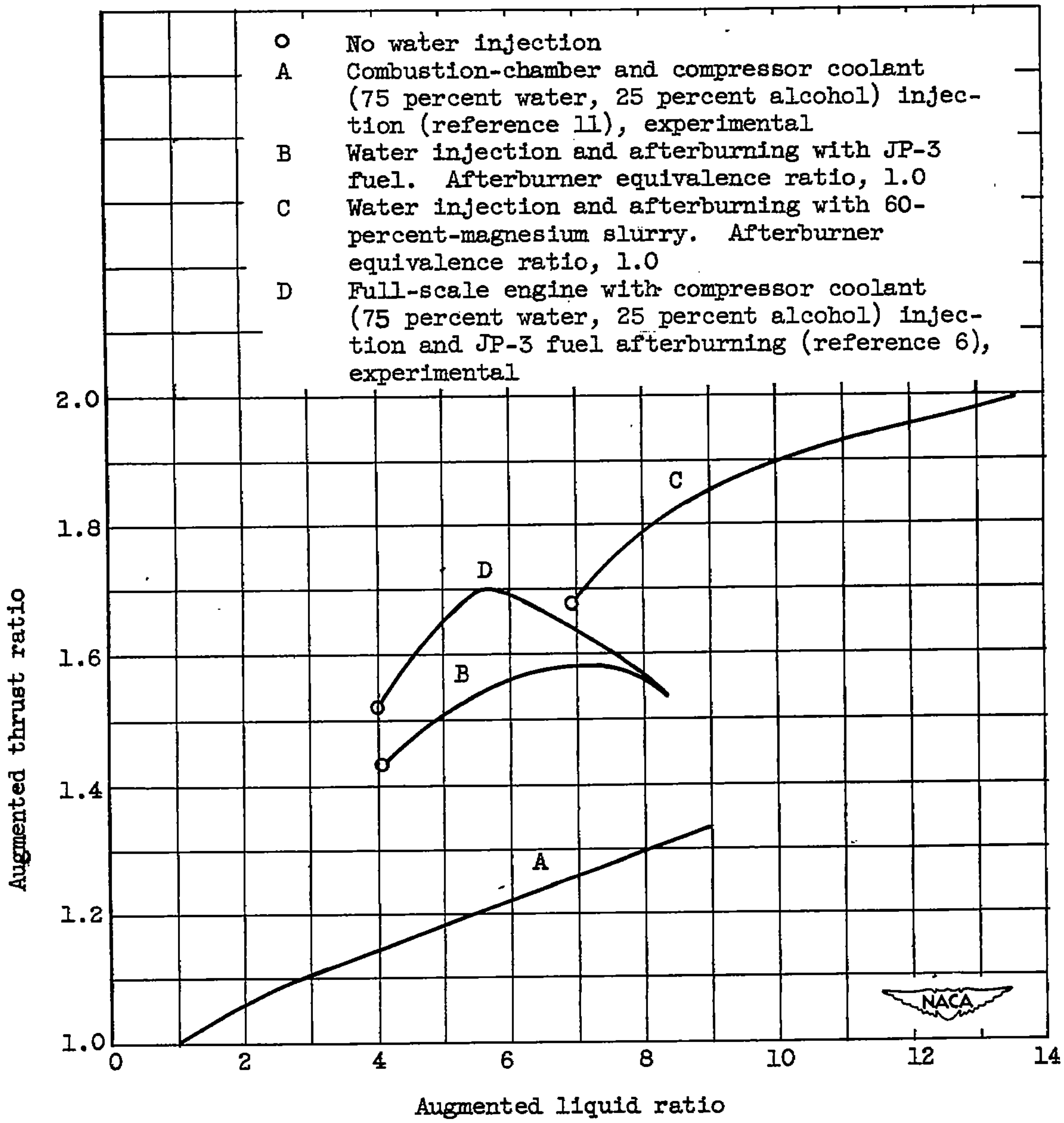


Figure 10. - Static sea-level thrust augmentation of turbojet engine combining afterburning with experimental water-injection performance.

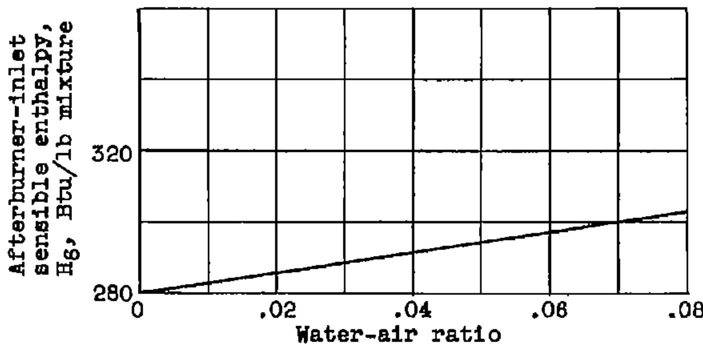


(a) Sensible enthalpy, above 537° R, of afterburner-inlet mixture containing products of propane combustion and water vapor at 1660° R, and JP-3 fuel at 537° R.

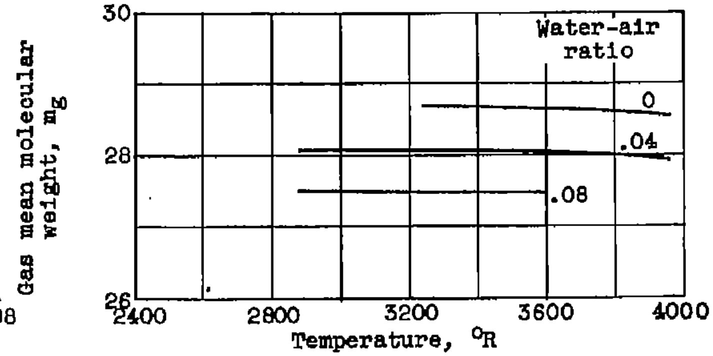


(c) Molecular weight of gaseous afterburner products.

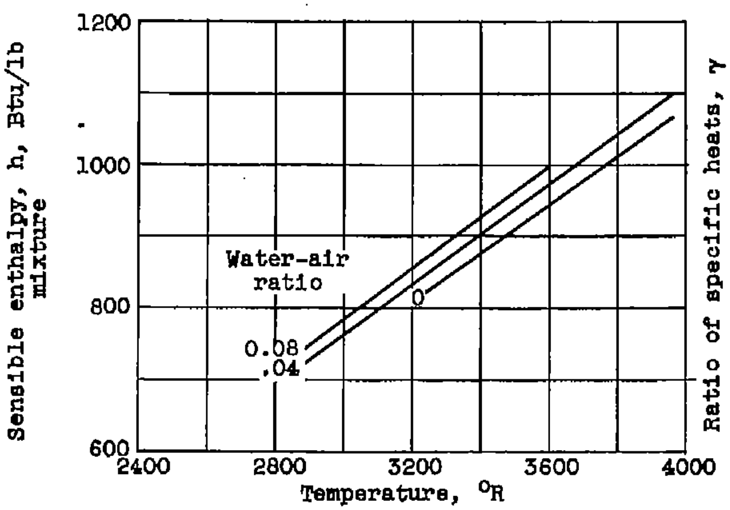


(b) Sensible enthalpy of afterburner products above 537° R.

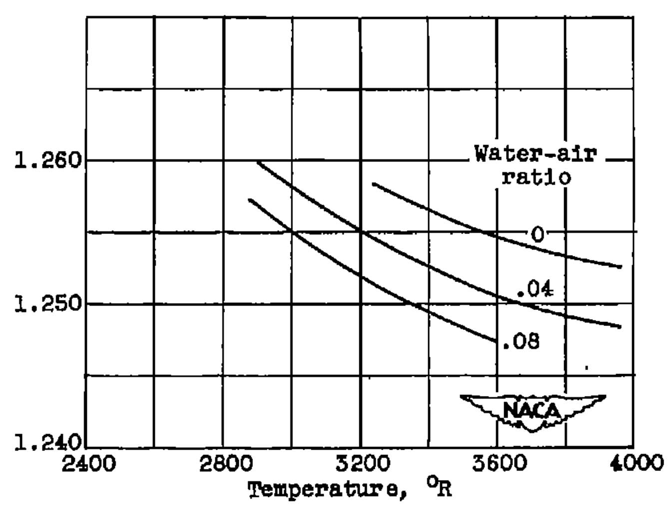


(d) Ratio of specific heats, $\gamma$.

Figure 11. - Thermodynamic properties of combustion products of propane and JP-3 fuel. Afterburner equivalence ratio, 1.0; assigned pressure, 2 atmospheres.

2568

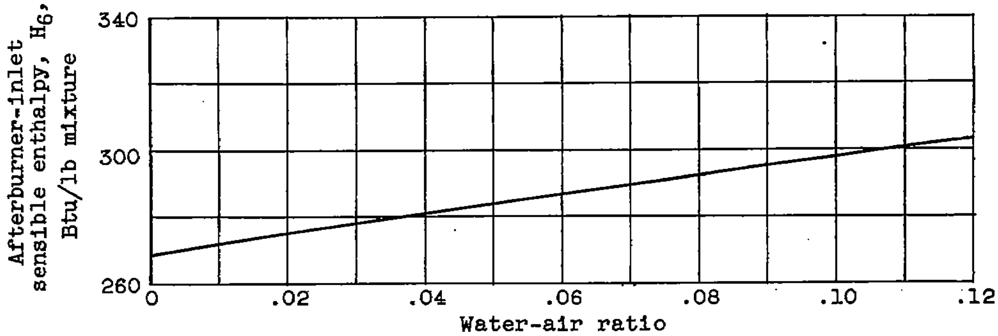


(a) Sensible enthalpy, above 537° R, of afterburner-inlet mixture containing products of propane combustion and water vapor at 1660° R, and magnesium slurry at 537° R.

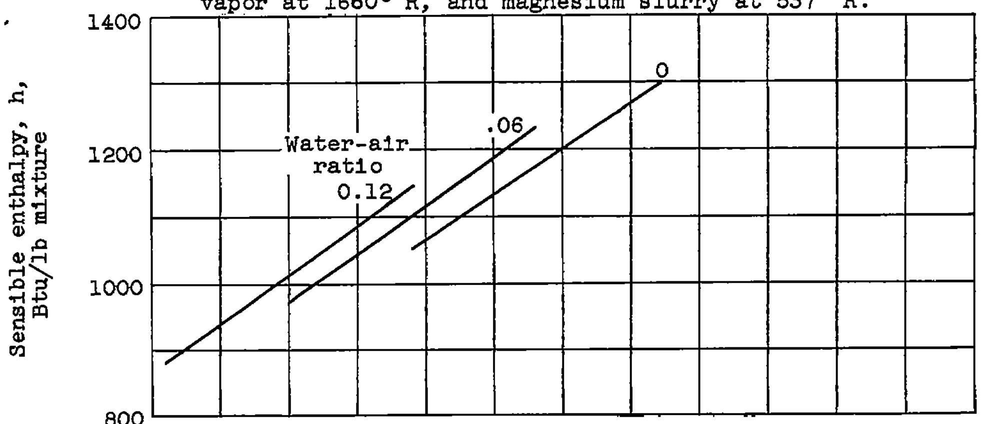


(b) Sensible enthalpy of afterburner products above 537° R.

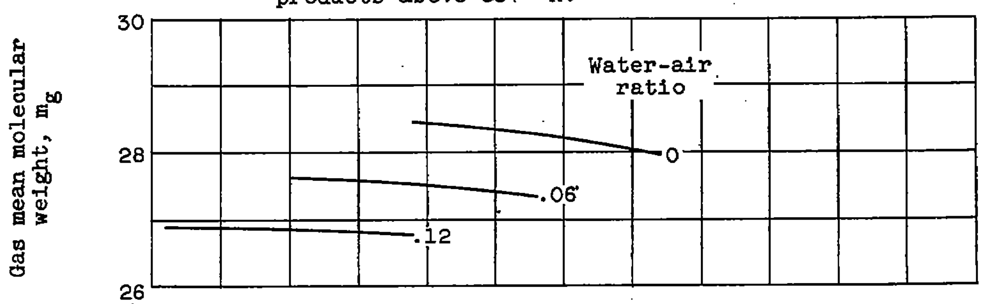


(c) Molecular weight of gaseous afterburner products.

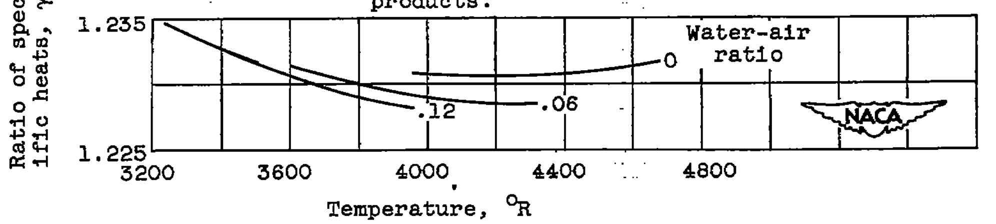


(d) Ratio of specific heats, γ.

Figure 12. - Thermodynamic properties of combustion products of propane and 60-percent-magnesium slurry. Afterburner equivalence ratio, 1.0; assigned pressure, 2 atmospheres.

2568

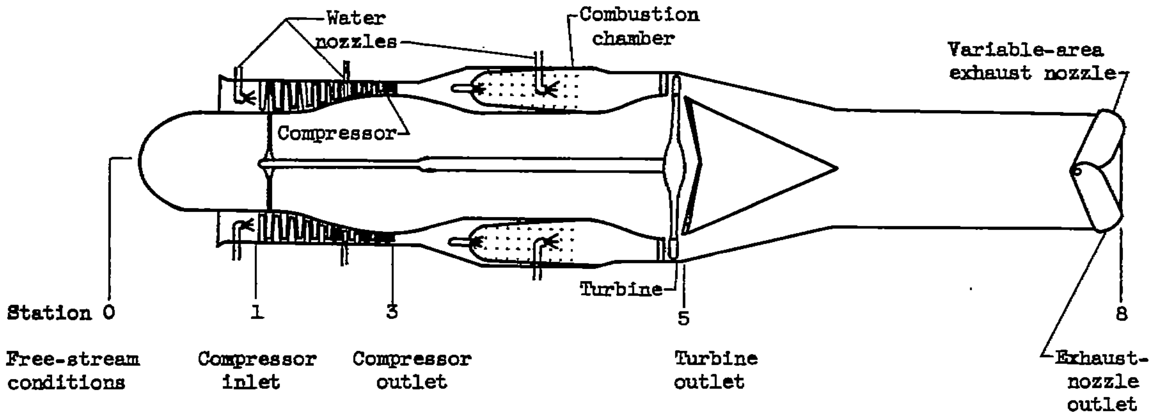


(a) Engine without afterburner.

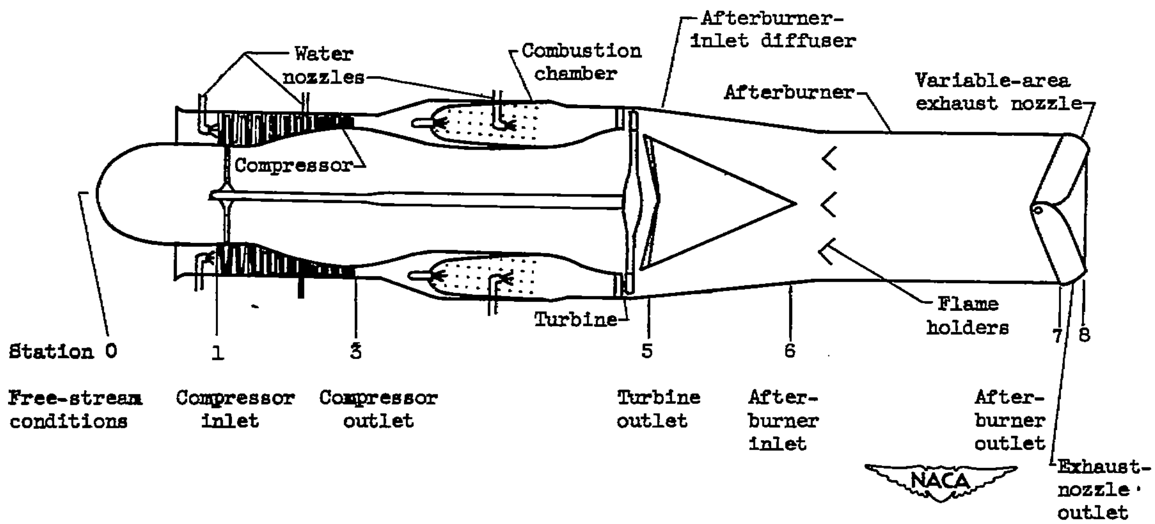


(b) Engine with afterburner.

Figure 13. - Schematic diagram of turbojet engine showing stations referred to in analysis of appendix D.

2568

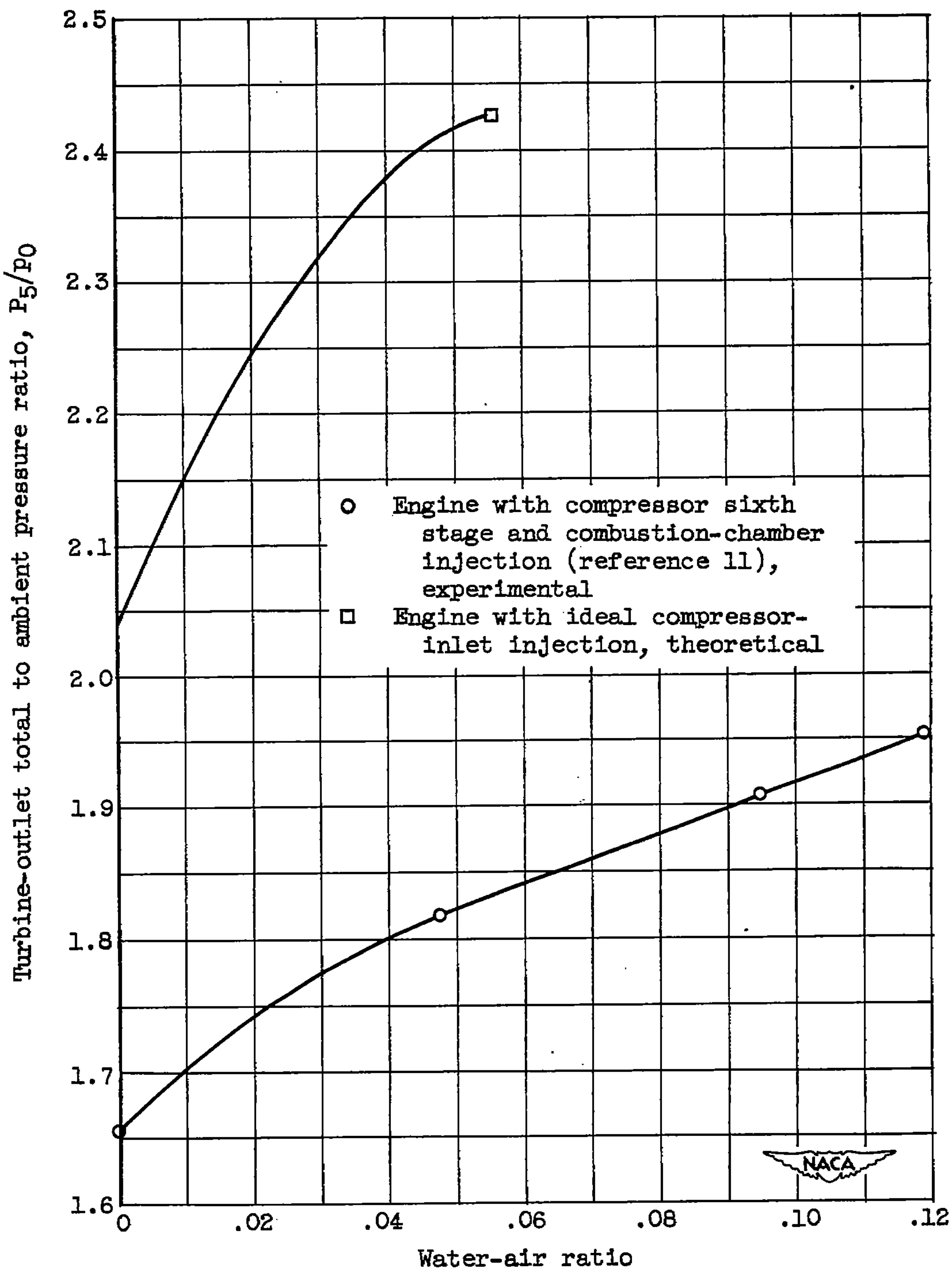


Figure 14. - Effect of water injection on turbine-outlet pressure ratio $P_5/p_0$ of turbojet engines. Normal compressor pressure ratio, 4.6.

2568

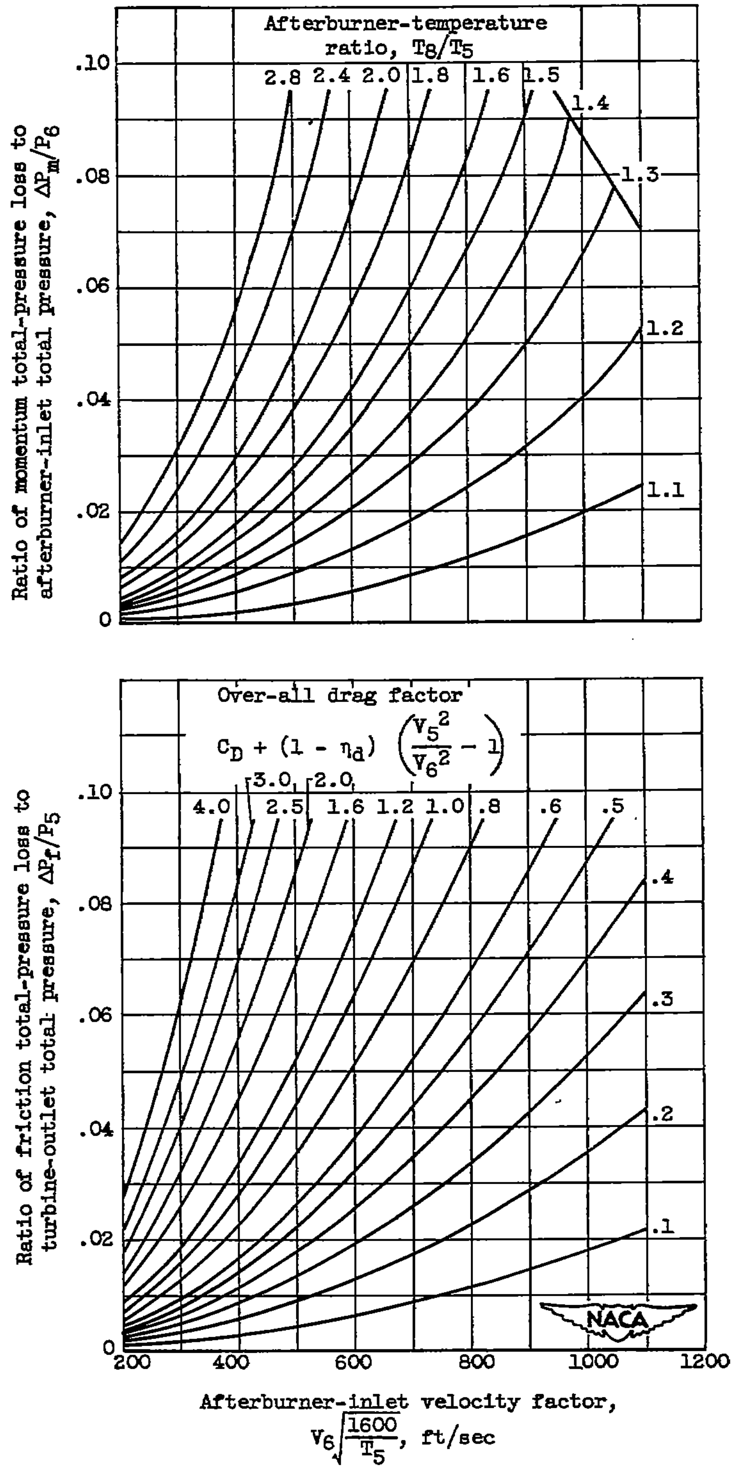


Figure 15. - Variation of friction and momentum total-pressure losses with afterburner-inlet velocity factor (reference 17).



NACA-Langley - 10-22-52 -350